Working Report 2007-81

Reactive Transport Predictions for an Olkiluoto Final Repository Tunnel Unit

Ari Luukkonen
Henrik Nordman

September 2007

POSIVA OY
Olkiluoto
FI-27160 EURAJOKI, FINLAND
Tel +358-2-8372 31
Fax +358-2-8372 3709

Working Report 2007-81

Reactive Transport Predictions for an Olkiluoto Final Repository Tunnel Unit

Ari Luukkonen

Henrik Nordman

Technical Research Centre of Finland (VTT)

September 2007

ABSTRACT

The presented hydrogeochemical reactive transport calculations concentrate to a defined unit piece (unit cell) of the planned Olkiluoto repository that is under design for spent nuclear fuel. The material properties assigned to the tunnel unit are based on literature as far as possible. Calculations make up geochemical future scenarios on the repository evolution. Most recent predictions on the potential future climate at Olkiluoto are utilised together with estimates how future hydraulic conditions affect the repository. Two climate scenarios are considered in detail. The Weichselian-R scenario is based on the repetition of the last glacial cycle, while the Emissions-M scenario attempts to predict the future groundwater conditions at Olkiluoto in the situation where the atmospheric greenhouse gasses delay the next glacial cycle at least for 100,000 years. The groundwater compositions, considered active at the repository depth in future, are judged in this study.

Several geochemical processes are considered active at the repository depth. Calculations concentrate on the changes occurring with time within the tunnel unit. All simulations are done in geochemically reducing conditions. It turns out that sulphur cycling in these conditions is in central role considering the safety assessment studies of Olkiluoto repository. Furthermore, groundwater salinity and cation occupancy within the exchange sites of montmorillonite contributes to sealing properties of the engineered barrier system.

Calculations attempt to estimate effects of possible future scenarios for the Olkiluoto repository. The results indicate that the buffer capacities assigned to the tunnel unit are large enough, at least to next 100,000 years, to maintain dissolved sulphide contents low in the groundwater infiltrating through the tunnel engineered barrier system. Geochemical reactions raise the bicarbonate levels within the groundwater. This is a useful buffer if low pH conditions emerge in the repository level. Calculations also predict the conversion of Na-montmorillonite to mixed (Na,Ca)-montmorillonite within the tunnel unit in 10,000–20,000 years from the start of the repository operations. This mineralogical change as well as salinity changes of infiltrating groundwater should affect the engineered barrier swelling pressures. However, pressure changes are not estimated in this study.

However, there are significant uncertainties included in the calculations. The future climatic and geological events are likely not completely understood. Groundwater flow/diffusion rates within the backfilled tunnel are uncertain. Changes in material properties (homogeneity, alteration) with time should be estimated as well.

Keywords: final repository, hydrogeochemistry, engineered barrier system, future scenario, geochemical mass-transfer, buffering capacity

Reaktiivisia kulkeutumisennusteita Olkiluodon loppusijoitustilan tunneliyksikölle

TIIVISTELMÄ

Esitetyt hydrogeokemialliset reaktiiviset kulkeutumislaskut keskittyvät rajattuun yksikköpalaan kaavaillusta Olkiluodon loppusijoitustilasta, jota suunnitellaan käytetylle ydinpolttoaineelle. Materiaaliominaisuudet, jotka on liitetty tunneliyksikköön perustuvat kirjallisuuteen niin pitkälle kuin mahdollista. Laskennat tekevät geokemiallisia tulevaisuusennusteita loppusijoitustilan kehityksestä. Mallinnuksissa hyödynnetään viimeisimpiä ennusteita siitä, miten mahdolliset Olkiluodon ilmastokehitysennusteet sekä mahdolliset tulevaisuuden hydrauliset olosuhteet vaikuttavat loppusijoitustilaan. Kahta ilmastoskenaariota tarkastellaan yksityiskohtaisesti. Weichselian-R ennuste perustuu viimeisen jääkausihistorian toistoon tulevaisuudessa. Toisaalta Emissions-M ennuste pyrkii ennustamaan tulevaisuuden pohjavesiolosuhteet Olkiluodossa tilanteessa, jossa ilmakehässä olevat kasvihuonekaasut viivästyttävät seuraavan jääkauden alkamista ainakin 100.000 vuodella. Loppusijoitussyvyydellä aktiivisiksi arvioidut pohjavesikoostumukset on päätelty tämän tutkimuksen yhteydessä.

Useat geokemialliset prosessit katsotaan aktiivisiksi loppusijoitussyvyydellä. Laskennat keskittyvät ajasta riippuviin muutoksiin tunneliyksikössä. Kaikki simuloinnit tapahtuvat geokemiallisesti pelkistävissä olosuhteissa. Tuloksista ilmenee, että rikin kierto näissä olosuhteissa on keskeisessä asemassa silmälläpitäen Olkiluodon loppusijoitustilan turvallisuusanalyysitutkimuksia. Lisäksi pohjaveden suolaisuudella ja montmorilloniitin kationimiehityksellä on vaikutusta rakennettujen päästöesteiden tiiviysominaisuuksiin.

Laskennoissa pyritään arvioimaan mahdollisten tulevaisuusennusteiden vaikutusta Olkiluodon loppusijoitustilaan. Tulosten perusteella näyttää, että tunneliyksikköön liitetyt puskurikapasiteetit ovat riittävän suuret vähintään seuraavan 100.000 vuoden ajan, että liuenneet sulfidipitoisuudet säilyvät alhaisina tunneliin rakennetun päästöesteen läpi suotautuvassa pohjavedessä. Geokemialliset reaktiot nostavat pohjaveden bikarbonattitasoa. Tämä on hyödyllinen puskuri, jos alhaisen pH:n olosuhteita ilmenee loppusijoitussyvyydellä. Laskennat myös ennustavat Na-montmorilloniitin muuttumisen sekoittuneeksi (Na,Ca)-montmorilloniitiksi tunneliyksikössä 10.000 – 20.000 vuoden kuluessa loppusijoituksen alkamisesta. Tällä mineralogisella muutoksella, kuten myös pohjaveden suolaisuusmuutoksilla pitäisi olla vaikutusta rakennettujen päästöesteiden paisumisominaisuuksiin. Näitä paisuntapaineiden muutoksia ei kuitenkaan arvioida tässä työssä.

Laskentoihin liittyy kuitenkin huomattavia epävarmuuksia. Tulevaisuuden ilmastollisia tai geologisia tapahtumia ei todennäköisesti täysin ymmärretä. Pohjaveden virtaus-/diffuusionopeudet uudelleentäytetyssä tunnelissa ovat epävarmoja. Ajasta riippuvat muutokset materiaalien ominaisuuksissa (homogeenisuus, muuttuminen) tulisi myös arvioida.

Avainsanat: loppusijoitustila, hydrogeokemia, rakennettu päästöestesysteemi, tulevaisuusennuste, geokemiallinen massa-siirtymä, puskurikapasiteetti

TABLE OF CONTENTS

1 INTRODUCTION

The geochemical reactive transport and cumulative mass-balance considerations made in this work focus on a small unit piece, referred hereafter as "unit cell", of the planned Olkiluoto repository. In principle, this unit cell can be replicated until essential parts of a complete repository are described. However, this step is not taken in the current study, but all results given are related to the single unit cell. The location of the unit cell is assigned to the middle of the first deposition tunnel of the planned final repository. In Figure 1-1, the first deposition tunnel can be found from the middle of the first construction stage of the repository.

The engineered barrier system (EBS) of the unit cell contains a backfilled tunnel unit and one canister hole. The canister hole contains one disposal canister and a tightly swelled bentonite buffer surrounding the canister. There may be moderate amounts of cement/concrete within the tunnel unit. For simplicity, the current calculations confine to the backfilled tunnel unit. Moreover, the possible high-pH conditions originating from degrading cement are discarded. Otherwise, the material properties given for the tunnel unit (physical and mineralogical) are based on literature values as far as possible. The chemical processes considered to be likely at the repository depth are dissolution/precipitation of certain minerals, cation exchange within clays, surface complexation (diffuse double layer approach), and certain microbially mediated chemical reactions.

Calculations concentrate to geochemical changes within the tunnel EBS as a function of time. The considered time-spans are extensive. Two climate scenarios are considered. Weichselian-R scenario is based on the repetition of the last glacial cycle. In the Weichselian-R scenario, the next glaciation will start about 13,000 years after the beginning of repository operations. Emissions-M scenario is based on moderate global emission estimate of greenhouse gasses (Cedercreutz 2004). At least during the next 100,000 years, no new glaciation will start in the Emissions-M scenario. The water compositions used in the two climate scenarios have been reasoned by utilising the available information from the Olkiluoto hydrogeochemical history, and the hydrological simulations done for the Olkiluoto site.

The simulations couple hydraulic groundwater flow through the unit volume to the geochemical reactions. The flow rates assigned to simulation steps are based on site scale hydraulic flow modelling estimates (Posiva 2007). However, the results of hydraulic flow simulations have been simplified, and judged reassessed values have been used in the hydrogeochemical couplings. Calculations integrate, over the simulation time-steps, the mass-transfers observed to occur within the tunnel unit. Results give estimates of net-transfers occurring e.g. as sulphate reduction and sulphide precipitation or as bicarbonate production within the tunnel unit. Results are used for estimations of the tunnel EBS buffer capacities.

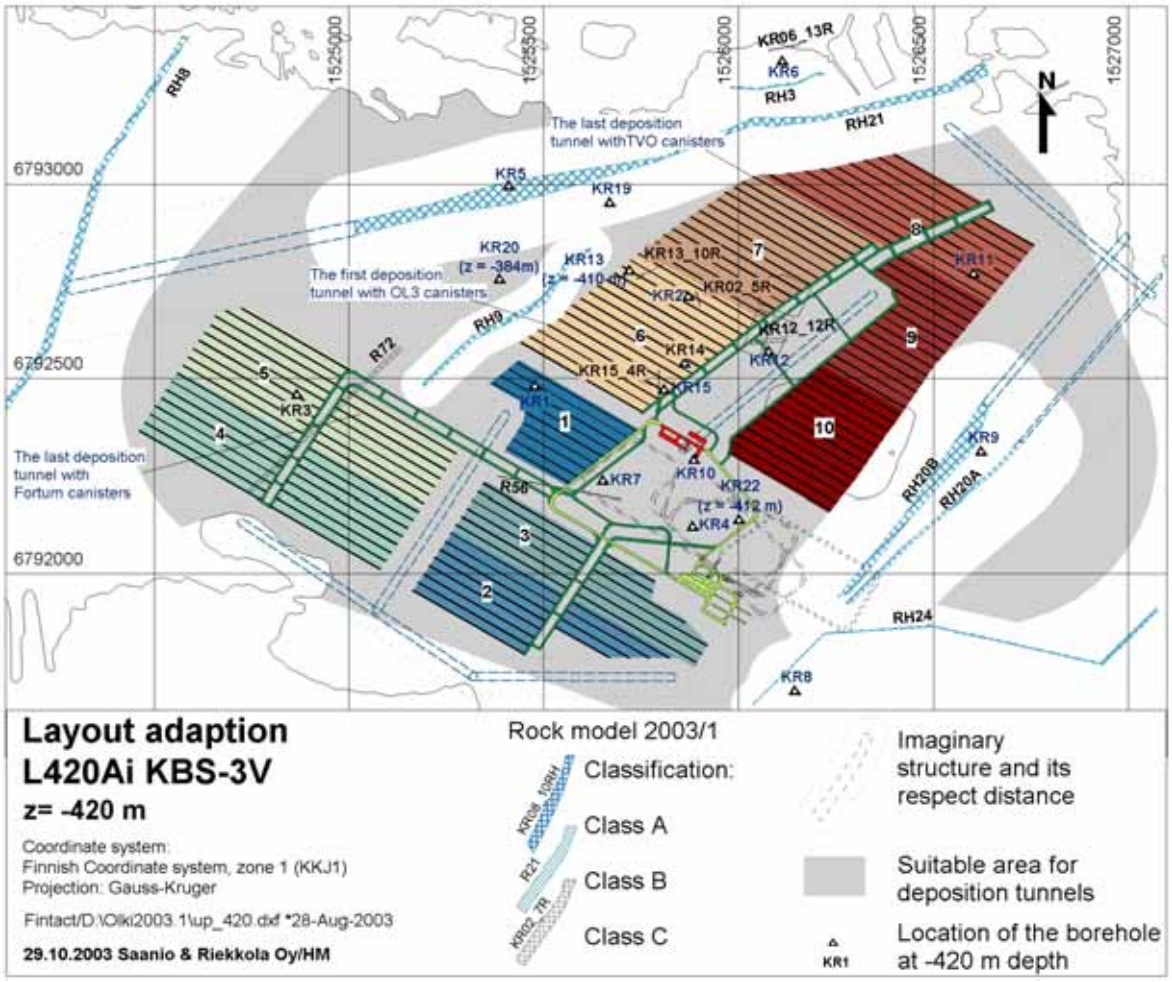

Figure 1-1. *An example of layout adaptation and construction stages of the repository at a depth of -420 m (Malmlund et al. 2004). The nine construction stages are also indicated.*

2 CONCEPTUAL MODEL AND CALCULATION TOOLS

To assess the geochemical environment of groundwater and solutes at the canister scale, the repository is conceptualized as series of unit cells. A unit cell comprises a section of the deposition tunnel (backfilled), the buffer and canister in the deposition hole (Figure 2-1).

The unit cell is composed of a 5.5-metre long section of tunnel (77 m^3) and of one deposition hole (19 m^3). The volume of the unit cell is 96 m^3. The tunnel backfill consists of 30% MX-80 sodium bentonite mixed with 70% crushed rock. The deposition hole contains the spent fuel canister and compacted bentonite blocks. For a full-scale test of the KBS-3V repository concept, Börgesson & Hernelind (1999) have estimated general physical properties for a tunnel backfill (Table 2-1).

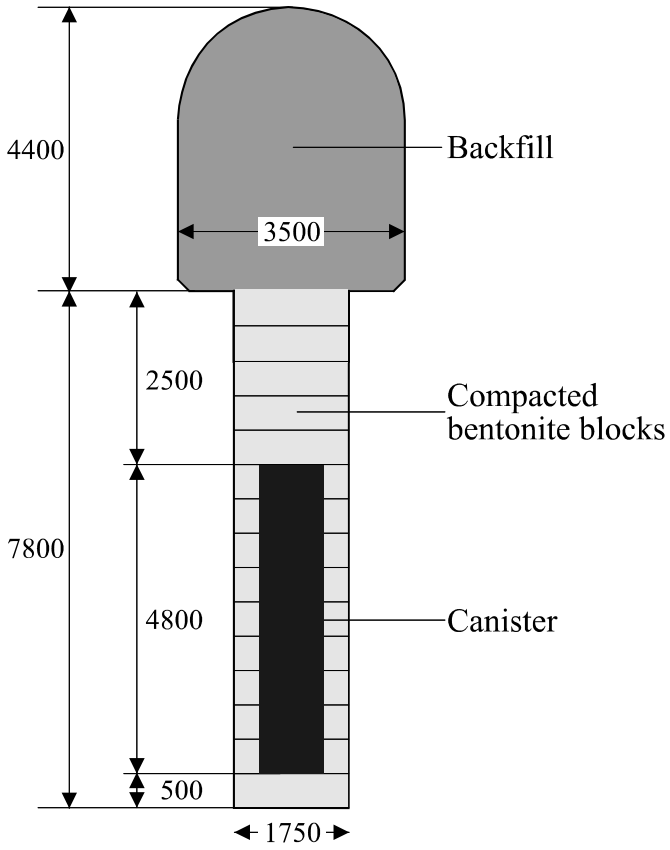

Figure 2-1. *Dimensions of the deposition hole and part of the deposition tunnel used in the conceptual model of the unit cell. All measures presented are in millimetres.*

Table 2-1. *Selected physical properties for initial compacted tunnel backfill in the Prototype repository (Äspö, Sweden). Parameters are after Börgesson & Hernelind (1999). Water content (m_{water}/m_{solid}), porosity (V_{void}/V_{tot}), and degree of saturation (V_{water}/V_{void}).*

Dry density g/cm^3	Water content	Porosity	Degree of saturation
1.75	0.19	0.363	0.58

According to the expected evolution, there will not be any advective transport inside the deposition hole, the only mass transport will occur via diffusion. Most of the geochemical reactions occur in the porewater of the backfill in the deposition tunnel, where some groundwater flow may occur. Therefore, the calculations presented here will concentrate to the tunnel backfill only.

The calculation tool for the geochemical evolution in the deposition tunnel is PHREEQC-2, a modelling tool developed by USGS (Parkhurst & Appelo 1999). In principle, PHREEQC-2 can be applied to simulate the chemistry in the deposition tunnel assuming that a diffusive flow of particles along the tunnel axis can be approximated with a slow advection. The code is capable of taking into account the advective transport of dissolved species undergoing chemical reactions in saturated groundwater system. The code capabilities include modelling of complex sets of reversible reactions, such as aqueous, mineral, gas, solid-solution, surface-complexation, and ion-exchange equilibria, and irreversible reactions, such as specified mole transfers of reactants, kinetically controlled reactions, and mixing of solutions. The results obtained with PHREEQC-2 are comparable with those obtained with another coupled reactive transport calculation tool, TOUGHREACT (Luukkonen et al. 2004; Luukkonen 2006).

It is assumed that bentonite utilised in the tunnel EBS is MX-80 sodium bentonite. The estimated average composition of tunnel backfill is presented in Table 2-2. From this set of minerals, the following are considered reactive in the current study: quartz, calcite, kaolinite, pyrite, gypsum, goethite, and amorphous iron. However, amorphous iron is a metastable mineral phase, and tends to recrystallise as goethite. These two mineral phases were summed up as goethite in the calculations. Finally, halite has been discarded from the equilibrium phases because its concentration within the backfill is minimal. Geochemical mass balance calculations have been carried out for both the Weichselian-R and the Emissions-M scenarios.

Advective transport of groundwater and solutes is not expected in the deposition hole. Once the buffer has reached its swelling pressure in the deposition hole, it will oppose the circulation of water and any groundwater and solute transport is expected to occur via diffusion. Due to high swelling pressures, little or no free (electroneutral) porewater is expected, but diffusion is assumed to occur mostly or completely through charged pores. This process is related to surface complexation and described in more detail below (Section 3.2). PHREEQC-2 (nor TOUGHREACT) is not designed for transport simulations of non-neutral waters or to maintain correct charge imbalances in waters during simulations. Another modelling tools that neglect intrinsic water chemical couplings (i.e. water chemical speciation and thermodynamic balances in water-rock

interaction) are needed for modelling the deposition hole (see e.g. Nordman & Vieno 2003). These calculations are not considered in this study, but the approach can be found e.g. from the study on the expected repository evolution (Posiva 2007).

The current study also assumes that important organic processes related to methane and organic matter oxidation, and to sulphate reduction are active in the tunnel backfill (Sections 3.3 and 3.4). Based on experimental results the viability of micro-organisms within the fully saturated deposition hole has been questioned (Karnland et al. 2000). The considerations of biohydrogeochemical processes within the saturated deposition hole are beyond the scope of this study.

Table 2-2. *Potentially reactive solids of the Olkiluoto repository tunnel backfill.*

Mineral (general formula given only for main minerals)	Unit wt g/mol	Rock muck[a] mol/kg	Bentonite[b] mol/kg	70/30 Backfill mol/kg	70/30 Backfill mol/(1L water)
Quartz (SiO_2)	60.1	3.87	1.66	3.21	35.0
Albite	262	0.72	0.27	0.59	6.39
K-feldspar	277	0.62	-	0.43	4.71
Biotite	456	0.46	-	0.32	3.53
Montmorillonite	744	-	1.01	0.30	3.30
Sillimanite	162	0.33	-	0.23	2.52
Cordierite	614	0.14	-	0.10	1.06
Sericite/illite	398	0.07	0.05	0.07	0.721
Calcite ($CaCO_3$)	100	0.01	0.14	0.05	0.549
Kaolinite ($Al_2Si_2O_5(OH)_4$)	258	-	0.15	0.05	0.506
CH_2O	30.0	-	0.13[c]	0.04	0.435
Pyrite (FeS_2)	120	0.02	0.03	0.02	0.265
Chlorite/Hornblende	619	0.02	-	0.02	0.172
Zircon	183	0.01	-	0.01	0.112
Gypsum ($CaSO_4$)	136	-	0.02[d]	0.01	0.077
Goethite (FeOOH)	88.8		0.02[d]	0.00	0.050
Epidote/Saussurite	469	0.01	-	0.00	0.046
$Fe(OH)_3$ (amorphous)	107		0.01[d]	0.00	0.035
Apatite	482	0.00	-	0.00	0.012
Garnet	489	0.00	-	0.00	0.007
Halite	58.4		1.35E-3[d]	4.05E-4	4.41E-3
Cation occupancies in the exchange sites[e]					
Na^+			0.67	0.20	2.18
Ca^{2+}			0.03	0.01	0.108
Mg^{2+}			0.02	0.01	0.065
K^+			0.01	0.00	0.043
Surface site capacity[f]					
S_wOH			0.03	0.008	0.092

[a] *General mineral composition after Vuorinen et al. (2003).*
[b] *General mineral composition after Bruno et al. (1999), and Bradbury & Baeyens (2002).*
[c] *Organic matter concentration after Pirhonen (1986), and Bradbury & Baeyens (2002).*
[d] *FeOOH, $Fe(OH)_3$, and NaCl concentrations after Bradbury & Baeyens (2002).*
[e] *Exchange site occupancies after Bradbury & Baeyens (2003).*
[f] *Amount of proton exchange sites after Wieland et al. (1994).*

3 HYDROGEOCHEMICAL MODEL FOR THE TUNNEL BACKFILL

The conceptual model used for geochemical calculations in the tunnel part of the unit cell considers slow advective/diffusive groundwater flow along the repository tunnel axis. The mass exchange calculations integrate the net-transfers observed in the outflow end of the tunnel unit. The mass exchanges are calculated in two steps. First, mass-transfers are accumulated and porewater composition changes are observed while an individual volume of water from the inflow side infiltrates through the tunnel unit. Second, mass-transfers are accumulated over the selected hydraulic time periods while the groundwater composition at the inflow side of the tunnel unit remains constant. In practice, calculations are done as follows. The tunnel unit is divided into 400 columns, and each tunnel backfill column is divided into 29 cells. Calculations are done for one backfill column and the results are multiplied by 400. In a backfill column porewater parcels are transported through successive backfill cells. An illustration of the modelling is presented in Figure 3-1. The calculation starts from the left (cell #1). Water remains in a cell until the residence time (a function of flow rate) is reached and then the water is transported into next cell further along the tunnel backfill column. The size of an individual tunnel backfill cell is 6.56 dm^3 assuming a porewater volume of 1 dm^3 and a porosity of 0.15 (Luukkonen 2004). The cell is a cube with an edge length of 0.187 metres. The calculation implements the pure 1-D advection without any side diffusion, but can be conceptualised as pure 1-D diffusion as well, though the hydrochemical coupling is done with advection equations.

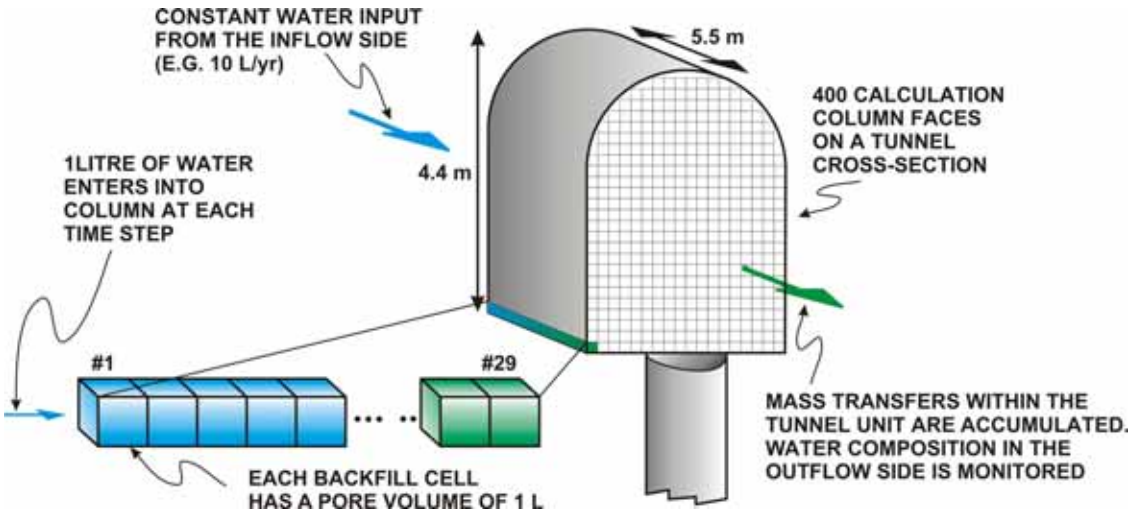

Figure 3-1. *Illustration of the conceptual model of the tunnel backfill part of the unit cell. Infiltrating water moves along the 5.5 metre-long tunnel section of the unit cell. The volume of the tunnel unit is divided into 400 columns. Each calculation column is divided into 29 cells. Material properties for each cell are considered as known parameters (i.e. amounts of reactive materials, cation exchange capacity, and 1-litre pore volume). The volumetric flow rate is assumed to be distributed homogeneously over the tunnel cross-section. Therefore, the flow rate within one calculation column is 1/400th of the total volumetric flow (e.g. 10 [L/yr] / 400 = 0.025 [L/yr] in one calculation column).*

The length of the tunnel in the unit cell (5.5 metres) was chosen because it corresponds to half the distance between two deposition holes (for OL-1 and OL-2 type of waste). If water is transported along the tunnel axis, the section of the tunnel in the unit cell contains 29 successive cells (Figure 3-1). The cross-section of repository tunnel is 14 m^2 while the area of an individual reaction cell face is 0.035 cm^2. In all, approximately 400 cell-columns are needed for filling up the tunnel part of the repository unit. The complete pore volume in the tunnel unit is 11,600 litres (11.6 m^3).

The assumption that water flows along the tunnel axis is simplistic, as other directions are also possible. However, the hydraulic conductivity measurements from a full size tunnel backfilling experiment indicate that hydraulic conductivities within the compacted backfill are clearly higher than within the surrounding normally fractured bedrock (SKB 2005). Therefore, it is likely that water will flow axially along the tunnel. Moreover, the tunnel backfilling experiment (SKB 2005) indicates that hydraulic conductivities within the tunnel backfill vary significantly. The central parts of the tunnel backfill are less conductive than the parts closer to tunnel walls. Finally, the calculation approach yields feasible estimates of the mass transfers irrespective of the direction of flow: considering the dimensions of the unit cell (Figures 2-1 and 3-1) the distances from the top to the bottom (4.4 metres), and from the side wall to the other (3.5 metres) of the tunnel unit are almost the same as the length of the tunnel unit (5.5 metres).

The main geochemical processes occurring in the backfill bentonite are mineral equilibria, cation exchange (in particular sodium and calcium), surface complexation, sulphate reduction, and anaerobic organic matter and methane oxidation.

3.1 Mineral equilibria

The average mineral composition of the tunnel backfill is presented in Table 2-2. The following minerals present in crushed rock/bentonite mixture are considered reactive in the current study: quartz, calcite, kaolinite, pyrite, gypsum, and iron (amorphous iron and its recrystallised form, goethite).

3.2 Cation exchange and surface complexation

The thermodynamic constants for cation exchange equilibria are presented on Table 3-1. The exchange site occupation at initial conditions is presented in Table 2-2. The cation exchange equilibria are after Wieland et al. (1994), though there are newer thermodynamics available (Bradbury & Baeyens 2003, 2002). Sensitivity calculations were carried out with both the thermodynamic data after Wieland et al. (1994) and Bradbury & Bayens' data. The results were very similar but the Wieland's modelling approach is simpler to handle so Wieland et al. data were used in this study.

Table 3-1. *Exchange and surface parameters for the thermodynamic models considered.*

Parameter	Reaction	Value
Cation exchange[a]		
log*K*	$Ca^{2+} + 2NaX \Leftrightarrow CaX_2 + 2Na^+$	0.21
log*K*	$Mg^{2+} + 2NaX \Leftrightarrow MgX_2 + 2Na^+$	0.13
log*K*	$K^+ + NaX \Leftrightarrow KX + Na^+$	0.26
Surface complexation[b]		
log*K*	$\equiv S^WOH + H^+ \Leftrightarrow \equiv S^WOH_2^+$	5.4
log*K*	$\equiv S^WOH \Leftrightarrow \equiv S^WO^- + H^+$	-6.7

[a] According to Wieland et al. (1994), Gaines-Thomas convention.
[b] According to Wieland et al. (1994)

The modelling of surface complexation follows the theory of diffuse double layer (DDL) model (e.g. Stumm 1992) and adapts the approach presented by Wieland et al. (1994). The thermodynamic equilibria are presented in Table 3-1. The amount of complexation sites is presented in Table 2-2. The protonation/deprotonation of a pH-dependent surface affects the surface charges of solids. At near neutral pH, it is expected that wet clay mineral surfaces (i.e. montmorillonite, kaolinite, and illite) become slightly negatively charged (cf. Appelo & Postma, 1996; Davis & Kent, 1990). The porewater in the diffuse layer is positively charged and this charge is proportional to distance from the platelet surface (see Figure 3-2).

The negative surface attracts dissolved cations but diffusion tries to push cations towards lower concentrations (i.e., towards the electroneutral porewater). Similarly, diffusion attempts to push anions towards the surface, but the charged surface repels anions. The thickness of diffuse layer is simulated using the Debye length ($1/\kappa$) approach (c.f. Appelo & Postma 1996):

$$1/\kappa = \sqrt{\frac{\varepsilon \cdot RT}{2(N_a q_e)^2} \cdot \frac{1}{1000 \cdot I}} \quad , \qquad \text{(Equation 3-1)}$$

where ε = dielectric constant for aqueous porewater (F m^{-1}), R = gas constant (J K^{-1}·mol^{-1}), T = temperature (K), N_a = Avogadro's constant (mol^{-1}), q_e = charge of proton (C), and I = ionic strength of porewater (eq kgw^{-1}).

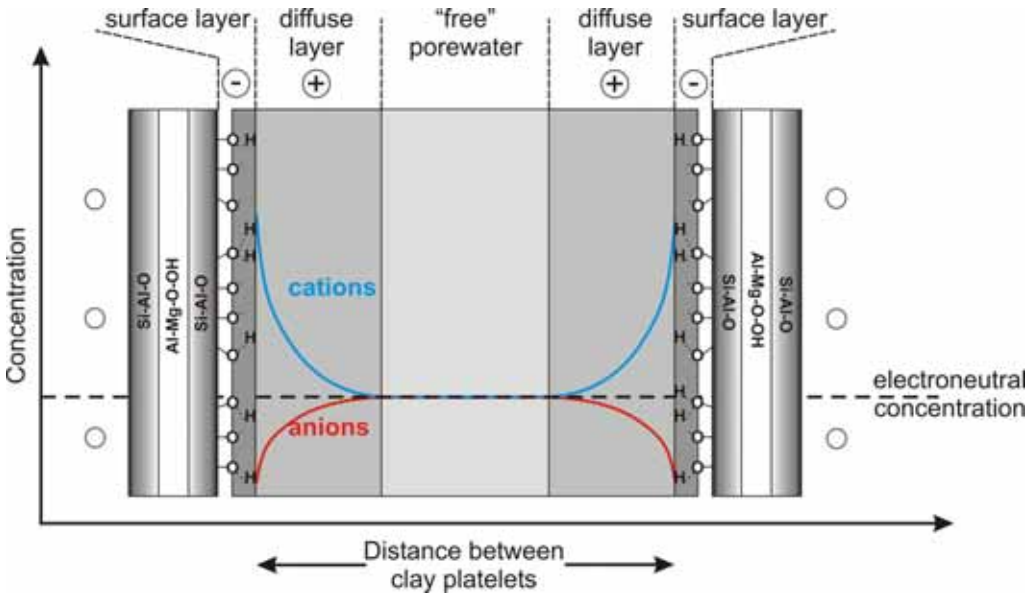

Figure 3-2. *Schematic distributions of cations and anions within the tunnel backfill pores. Surface layers are negatively charged, diffuse layers are positively charged, and free porewater is electroneutral.*

As an example, water with a TDS of 20 g/L and an ionic strength 0.43, at 40 °C, has a Debye length of approximately 5Å. The Debye length approximately doubles if the ionic strength drops by one fourth (i.e. an ionic strength of 0.1 corresponds to a Debye length of 10Å). The thickness of diffuse layer affects the pore volume available for "freely" movable water (and correlates with the swelling pressure of backfill). In the calculations, however, diffuse layers are considered only to maintain charge balance in the porewater. I.e. diffuse layers do not diminish (as they should) the 1dm^3 pore volume designed available for input water within each calculation cell.

3.3 Sulphate reduction

Important features of the tunnel unit are related to SO_4^{2-} and HS^- considerations. Significant concentrations of hydrogen sulphide may accelerate canister corrosion because HS^- is highly reactive with metals. Sulphate reduction by organic matter is catalysed by sulphate reducing bacteria (SRB). The simplified overall reaction for this process can be presented as follows:

$$CH_2O + 0.5SO_4^{2-} \rightarrow HCO_3^- + 0.5H_2S\,. \qquad \text{(Equation 3-2)}$$

In Equation (3-2), CH_2O is a simplified form of metabolizable organic matter. The initial reactivity of organic matter depends on number of factors. In addition to carbon, organic matter probably contains variable amounts of nitrogen and phosphorous groups.

Chemical bonds within carbon chains vary, chains differ in length, and chains likely contain variable active species, e.g. -COOH, -CH_2OH, etc.

In anoxic sea bottom sediments, this is a major process causing organic degradation. Several sulphate reduction studies related to the sea bottom sediments have been carried out (e.g. Roychoundhury et al. 2003, Koretsky et al. 2003, Van Cappellen & Wang 1996, Boudreau & Westrich 1984). It is reasonable to assume that processes within crystalline bedrock are similar. The modelling of anaerobic oxidation of organic matter is usually solved by using the Monod reaction rate law:

$$R_{SO_4} = R_{\max} \frac{[SO_4]}{K_{SO_4} + [SO_4]} = k_{SO_4} [CH_2O] \frac{[SO_4]}{K_{SO_4} + [SO_4]} , \qquad \text{(Equation 3-3)}$$

where R_{max} is the maximum rate (mol m^{-3} s^{-1}), and K_{SO4} is the half saturation concentration of sulphate (M), and k_{SO4} is the first-order rate coefficient (s^{-1}) of carbon oxidation. Equation (3-3) indicates that when the sulphate concentration becomes high enough, the rate of oxidation of organic matter becomes independent of the availability of sulphate. Conversely, below a critical level, the availability of sulphate becomes rate-limiting.

According to Appelo & Postma (1996), measured rates of organic degradation vary over several orders of magnitude. For example, in a saltmarsh sediment the first order rate coefficients (k_{SO4}) seem to vary at least in the range from $1.1 \cdot 10^{-9}$ s^{-1} to $6.5 \cdot 10^{-10}$ s^{-1} (Roychoundhury et al. 2003, 1998), while the half saturation concentration (K_{SO4}) varies around 240–204 µM. On the other hand, organic degradation rate by sulphate reduction in a meromictic lake bottom sediments give rate coefficient (k_{SO4}) estimates of the order $2.5–9.5 \cdot 10^{-14}$ s^{-1}, with half saturation concentrations at a range of 250–370 µM (Viollier et al. 2000).

In this study, the kinetic constraints for organic matter consumption were set to low values (i.e. $k_{SO4} = 1.0 \cdot 10^{-13}$ s^{-1} and K_{SO4} =250 µM) to provide a relatively slow input sulphate reduction rate.

3.4 Anaerobic methane oxidation

The mechanism of anaerobic methane oxidation is not well understood, and extensive microbiological research is ongoing to find the organisms that are responsible for anaerobic methane oxidation. The net-reaction for anaerobic methane oxidation can be represented by the equation:

$$CH_4 + SO_4^{2-} \rightarrow HCO_3^- + HS^- + H_2O , \qquad \text{(Equation 3-4)}$$

Valentine & Reeburgh (2000) proposed that a primitive single celled group of bacteria (methane oxidising Archaea) produce acetate from CH_4 and CO_2. Alternatively, the methane-oxidising Archaea could possibly produce acetate and H_2 by digesting only CH_4. The reaction products (acetate and H_2) are utilised by the SRB that produce bicarbonate and hydrogen sulphide as reaction product. The complete process (Eq. 3-4) involves both methane-oxidising bacteria (Archaea) and SRB.

The microbially mediated methane oxidation, as well as the methane producing metabolism (methanogenesis), is important component of carbon cycling in anaerobic environments. It was long considered that methanogenesis is a terminal step in the ecological carbon flow. However, over the last decades there has emerged compelling evidence that the anaerobic methane oxidation in various geological environments (e.g. marine and continental margin sediments) is of global significance (Valentine & Reeburgh 2000). Still, the mechanism of anaerobic methane oxidation is not well understood, and extensive microbiological research is going on (e.g. Girguis et al. 2003) in order to find the organisms that are responsible for the net-reaction (Equation 3-4).

In the case of organic matter oxidation, SRB produce HS^- directly from organic matter and sulphate (Equation 3-2). Anaerobic methane oxidation requires an association of Archaea and SRB for production of HS^- (Equation 3-4). Conceptually, methane oxidation is likely a two-step biochemical process where the former process remains exergonic (Archaea digestion) if the latter process digests the reaction products of the former. Intuitively, it seems that the organic matter consumption is the principal consumer of dissolved sulphate overriding the methane oxidation as long as there is digestible organic matter available.

3.5 Site-scale groundwater flow modelling

The site-scale modelling of groundwater flow, solute transport and heat transfer obtained from site-scale modelling (Posiva 2007) provides input data for the canister-scale mass balance calculations at different times: groundwater flow (in the form of Darcy velocity), salinities and temperatures in the tunnel backfill. One of the main uncertainties in the input data is the groundwater flow rate in the tunnel backfill.

The groundwater flow calculated with site-scale groundwater simulations is conceptually different from the groundwater flow in a deposition tunnel. In the former the bedrock is treated conceptually as an “equivalent porous medium” ignoring the effects of the EDZ and the backfill of the tunnel, i.e. similar hydraulic properties to those before the excavation are assumed for the closed tunnels. The groundwater flow in the deposition tunnel is subjected to local variations of the flow due to the existence of an EDZ or other preferential flow paths along the deposition tunnel or the proximity of a sparsely fractured zone. The high variability in groundwater flow at repository scale was discussed in Poteri & Laitinen (1999).

Nonetheless, lacking better data on groundwater flow in the canister surroundings and neighbouring tunnel, the site-scale flows can provide an indication of the trends of groundwater flow during the evolution time spans. The site-scale groundwater flow calculations provide a Darcy velocity, which is converted into a flow rate by multiplying it by the tunnel area (14 m^2). The range of Darcy velocities calculated at the

site-scale ranges from $1.1 \cdot 10^{-4}$ m/year during the excavation phase to $7 \cdot 10^{-7}$ m/year during the post closure phase and down to $3.5 \cdot 10^{-8}$ m/year during the far future phase in presence of a stationary ice sheet. The corresponding flow rates in the tunnel unit cross-section (14 m^2) would be 1.5 L/year during the excavation phase, and 9.8 mL/year and 0.5 mL/year during the post-closure and far future phases, respectively.

Such flow rates are not considered representative of the actual canister-scale flow rates because they are averaged over the entire site. Furthermore, the site-scale model assumes that the hydraulic conductivity of both the sparsely fractured rock and backfill are the same ($3 \cdot 10^{-12}$ m/s). However, according to measurements in the Backfill and Plug Test at Äspö, the hydraulic conductivity (K) within a fully saturated backfill (assuming a mixture of 30% bentonite and 70% crushed rock) varies from the proximity of tunnel walls to the central parts of tunnel from $5.0 \cdot 10^{-8}$ m/s to $1.4 \cdot 10^{-9}$ m/s, respectively (SKB 2005, p. 49). The difference in conductivity depends on the compaction of the backfill; but it also indicates that, despite efforts, the conductivity in the backfill remains higher than that of the host rock.

As an alternative theoretical approach it can be considered that the streamlines of groundwater flow are collected from a width of 25 metres (distance between deposition tunnels) and height of e.g. 100 metres. This would mean that the flow into tunnel would be collected from an area about 180 times the area of the tunnel (14 m^2). A further argument to reconcile the groundwater flow through a deposition tunnel with that at the site-scale is to calculate the flow using the Carslaw & Jaeger (1959) formula. The gradient in a well conducting ellipsoid (e.g. a tunnel) located in a homogeneous material may be obtained according to Equation 3-5:

$$V_F = V \cdot \left(1 + \frac{(K' - K)}{K} \cdot \frac{b^2}{a^2} \cdot (\ln(2a/b) - 1) \right)^{-1}, \qquad \text{(Equation 3-5)}$$

where V_F is the gradient in the ellipsoid (or tunnel), V is the gradient in the rock far away, K' is the conductivity (m s^{-1}) in the ellipsoid, K is the conductivity (m s^{-1}) in the rock, b is the half diameter (m) of the ellipsoid (or tunnel), and a is the half length (m) of the ellipsoid (or tunnel).

The parameter a is set to 150 metres (half of tunnel length of 300 m) and b is set to 4. The K' is assumed to be 100 or 1,000 times larger than K. The gradients in the tunnel (ellipsoid) would be from about 80 % to 30 % of that in the bedrock. Thus the flow rate in the tunnel would be between about 80 and 300 times higher than within intact rock. Based on these speculations, in the studies of the geochemical reactions in the tunnel backfill, the groundwater flow rate from the site-scale modelling is therefore multiplied by 1,000 to obtain a more suitable input flow rate in the tunnel part of the unit cell.

These groundwater flows are not to be considered representative of all unit cells in the repository. As mentioned before, a large variability of flow rate can be encountered in

different parts of the repository and therefore two unit cells may experience considerably different flow rates, depending on their position in the repository. The groundwater flows used in this study are therefore possible in a limited number of unit cells but are overall highly conservatives. In the normal evolution of the repository it is expected that the flows will be somewhere between the values calculated with the site-scale groundwater flow simulations and the values used in the present calculations.

Salinity levels in the unit cell are also obtained from the site-scale hydrogeological evolution of the geosphere (Posiva 2007). These values are used directly in the mass balance calculations because they are in the range of the observed salinities measured at repository depth. The absolute values of the salinity in one unit cell is also highly variable, as with the flow, therefore the values used for salinity levels are not necessarily representative of all unit cells. The chemical composition of the groundwater that enters the unit cell is directly derived or extrapolated from Olkiluoto samples. However, the metastable coexistence of methane and sulphate in the repository depth environment cannot be observed from the existing Olkiluoto groundwater samples. This redox pair will inevitably produce dissolved or precipitated sulphides in geological timescales (observed in real geochemical samples). Therefore, the simulated composition of the initial water input contains higher concentrations of hydrogen sulphide than the actual samples because microbially mediated methane oxidation is expected to occur. The final input water has also been equilibrated with calcite and pyrite that remove a part of dissolved bicarbonate and hydrogen sulphide from water.

The average temperatures in the tunnel part of the unit cell are derived from the calculated thermal evolution of the centre of the first deposition tunnel obtained with the "equivalent porous medium" concept (Posiva 2007). In this study, the selected temperatures correspond to the average temperatures over the time-periods studied. Again, average temperatures assigned for the centre of the first deposition tunnel are not always similar to temperatures simulated in the other parts of the repository.

4 GEOCHEMICAL MASS BALANCES IN THE TUNNEL BACKFILL

The parameters of interest are: pH, methane (CH_4), total dissolved solids (an approximate function of the concentration of chloride ions, Cl^-) as well as sulphates (SO_4^{2-}) and sulphides (HS^-). Sulphates and sulphides may be the two most important species from the canister durability perspective. The groundwater at Olkiluoto bedrock contains natural SO_4^{2-}. Dissolved sulphate can be reduced to dissolved hydrogen sulphide if conditions are suitable. The simulations consider two possibilities for sulphate reduction. Firstly, sulphate reduction may occur by anaerobic methane oxidation (see Equation 3-4). Deep waters in Olkiluoto contain abundant methane gas. Secondly, sulphate reduction may occur by oxidation of organic matter (see Equation 3-2). Both processes are microbially mediated and produce hydrogen sulphide and bicarbonate (see below). Significant concentrations of hydrogen sulphide may accelerate canister corrosion because HS^- is highly reactive with metals, including copper.

4.1 Weichselian-R scenario

4.1.1 Input data from site-scale groundwater flow modelling

Data on groundwater flow, temperatures, and total dissolved solids in the unit cell have been extrapolated from the site-scale groundwater flow calculations (Posiva 2007). These values are presented in Table 4-1.

The hydraulic gradients can be evaluated to those obtained with the site-scale groundwater flow calculations by dividing the Darcy velocity (Table 4-1) by the hydraulic conductivity of the sparsely fractured rock at the repository level ($K=3.0\cdot10^{-12}$ m/s). For example, the average hydraulic gradient for both climate scenarios at t=1,000 years is 0.77%, which is in line with the calculated site-scale groundwater flow in Olkiluoto (Posiva 1999). For comparison purposes, the maximum gradient encountered near the surface (due to the topography) is of the order of 4-5%.

According to Table 4-1, e.g. after about 2,000 years, the average Darcy velocity would be $2.6\cdot10^{-14}$ m/s or $8.2\cdot10^{-7}$ m/yr in the tunnel. Correspondingly the flow rate through a tunnel area of 14 m^2 would be 0.011 l/yr. In the ground water flow analyses both for the sparsely fractured rock and closed repository tunnels a hydraulic conductivity of $3\cdot10^{-12}$ m/s was used. In this study, the value 0.011 l/yr has been considered simply too low value. Therefore, the utilised flow rates were reconciled as justified in Chapter 3.5. The average flow rates, salinity values and temperatures in the tunnel backfill used for geochemical mass balance calculations in the tunnel part of the unit cell at different time periods are presented in Table 4-2.

Based on the site-scale groundwater flow modelling, it is estimated that it takes approximately 100 years to recover slowly from the high flow rates induced by the excavation and operation of the repository. Thereafter, the changes in flow rates, salinity levels and temperatures are smaller. Thus, the post-closure phase is divided into four steps, as shown in Table 4-2. The period starting from the onset of the next glaciation is represented by two sets of data, one corresponding to the permafrost phase (13,000 to 35,000 years) and one corresponding to an ice-sheet phase (35,000-125,000 years). Within the glaciation period there can be glacial melting and submerged periods.

Table 4-1. *Data imported from site-scale groundwater flow calculations (Posiva 2007). Time from the beginning of depositions, Darcy velocities, TDS concentrations and temperature. Results refer to the Weichselian-R scenario.*

Time (yr)	Calculated Darcy velocity (m/yr)	Flow through an tunnel area of 14 m^2 (l/yr)	TDS (g/l)	Temperature (°C)
Operational phase				
0	$5.4 \cdot 10^{-4}$	7.6	10.8	
100	$1.1 \cdot 10^{-4}$	1.5	8.3	45.0
From closure to the next glaciation				
200	$5.4 \cdot 10^{-7}$	0.0076	8.2	44.5
300	$5.0 \cdot 10^{-7}$	0.0070	8.3	43.4
1,000	$7.3 \cdot 10^{-7}$	0.010	8.1	37.7
2,000	$8.2 \cdot 10^{-7}$	0.011	8.3	33.4
10,000	$1.1 \cdot 10^{-6}$	0.015	4.1	25.8
From the next glaciation to the far future				
13,000	$7.3 \cdot 10^{-7}$	0.010	11.3	20.0
15,000	$7.6 \cdot 10^{-8}$	0.0011	12.7	20.0
20,000	$6.9 \cdot 10^{-8}$	0.00097	15.3	20.0
30,000	$6.0 \cdot 10^{-8}$	0.00084	19.4	20.0
40,000	$4.4 \cdot 10^{-8}$	0.00062	22.8	20.0
50,000	$3.0 \cdot 10^{-8}$	0.00042	25.2	20.0

High uncertainties are associated with the hydraulic gradients caused by glacial melting. The flow rates during the ice margin melting, obtained through the site-scale modelling, indicate that the maximum Darcy velocity would be about $7.9 \cdot 10^{-6}$ m/yr (0.11 L/year or 110 L/y if multiplied by 1,000). However, based on the speed of a melting glacial margin moving over Olkiluoto Island (c.f. Posiva 2007), glacial melting events are short-lived (approximately 100 years) compared to changes in the transmissivity of bedrock fractures. Similarly, the TDS concentration at the repository level would change only a couple of percent during this period. Therefore, in this study the assumption is that the glacial melting period will not have any significant effect on the chemistry of the repository.

Table 4-2. *Time periods from start of operation, the chosen flow rates in the tunnel, and TDS concentrations for the Weichselian-R scenario.*

Time frame	Time (years after beginning of depositions)	Groundwater flow rate for the tunnel (L/yr)	TDS concentration (g/L)	Temperature in the backfill (^{o}C)
Operational phase	0-100	1,500	9	45
From closure until the next glaciation	100-200	10	9	45
	200-5,000	10	8	35
	5,000-10,000	10	5	28
	10,000-13,000	10	5	23
From the onset of the next glaciation until the far future	13,000-35,000	1	15	23
	35,000-125,000	0.5	25	20

During the submerged period, the groundwater flow values used for the ice-sheet period can be applied because of the lack of hydraulic gradients within the bedrock. The remaining phases of the glacial cycle (formation of an ice sheet, followed by melting and a submerged phase) are expected to be similar to the preceding ones. Therefore, input data for glacial melting phases and submerged phases are considered the same as those for the ice-sheet phase.

4.1.2 Operational phase

Based on hydrological simulations the salinity of groundwater is about 9 g/L and the temperature about 45°C in the middle of the first deposition tunnel (see Table 4-2). These conditions prevail in the first deposition tunnel after its closure and saturation, while operational stage continues in the other parts of the repository. The present calculations assume that the post-operational disturbed high-flow stage in the first deposition tunnel continues about 100 years after the first tunnel closure.

During the operational phase, the groundwater surrounding the repository will be likely composed of two sources: drawn-down water with a seawater affinity and up-coned saline water with coexisting gases. The water salinity of 9 g/L is built up from two actual Olkiluoto samples presented in Table 4-3. The initial average water is a weighted sum from the tabulated Olkiluoto samples. However, this water coexists with a methane phase that is not supposed to be stable with the dissolved sulphate. Therefore, the microbially mediated methane oxidation is postulated to occur. The reaction produces hydrogen sulphide in the final average input water. However, the reaction is not taken as an irreversible reaction and a small concentration of methane is left into water (Table 4-

3). The final input water has also been equilibrated with calcite and pyrite that remove a part of dissolved bicarbonate and hydrogen sulphide from water.

The calculated total mass-transfers during the repository operational stage are presented in Table 4-4. During the first 100 years, 150,000 litres (150 m^3) of water flow through the 5.5-metre long backfill part of the unit cell.

Calculations take into account mineral equilibria among quartz, calcite, kaolinite, pyrite, gypsum and goethite (cf. Table 2-2). Organic matter is consumed for sulphate reduction during calculations. Porewater compositions are also affected by cation exchange of montmorillonite, surface charges of montmorillonite, and counterbalancing diffuse layers upon clay surfaces (see Figure 3-2).

According to Table 4-4, a large amount of Na^+ is flushed out from the system. Ca^{2+} is entrapped within the exchange sites of the unit volume. However, the input water is not the only source of Ca^{2+}. All gypsum is dissolved quickly away from the unit volume. The produced Ca^{2+} is exchanged with Na^+ while a large part of dissolved SO_4^{2-} is flushed out from the unit volume. High dissolved sulphate concentrations also accelerate organic matter consumption somewhat. Consumption of organic matter produces dissolved hydrogen sulphide (HS^-) and hydrogen carbonate (HCO_3^-) into the porewater. However, the positive mass-transfer of HCO_3^- indicates that high SO_4^{2-} concentrations available (gypsum dissolution) stimulate organic matter consumption (Eq. 3-2). Furthermore, effective take-out of Ca^{2+} from the water stimulates calcite dissolution from the tunnel backfill.

During the first 100 years montmorillonite within the tunnel unit looses a part of its Na-montmorillonite character. However, by the end of simulation calculations, the molar ratios of exchangeable cations within montmorillonite of the last calculation cell (cell #29, cf. Fig. 3-1) are: NaX = 0.79, CaX_2 = 0.16, MgX_2 = 0.04, and KX = 0.02. I.e. Na-montmorillonite composition is still untouched in the last calculation cell.

All HS^- from the constant input (Tables 4-3 and 4-4) is precipitated within the unit volume. The reaction occurs with goethite dissolution producing dissolved iron. Consequently, the precipitation of pyrite becomes possible. Due to iron speciation in the reduced conditions small amount of dissolved iron is flushed out of the unit volume.

Table 4-3. *Compilation of model input water with salinity of 9 g/L (see Table 4-2). The initial waters have been chosen from the Posiva's OIVA (KR1_T612_2 saline), and from VLJ (OL-PVA3, 7.7.1999) databases. The saline OIVA sample coexists with a gas phase containing approximately 270ml/L(H_2O) methane. The initial average water is a weighted sum. The final average input water has been modified from the initial average with methane oxidation reaction coupled with calcite and pyrite equilibria.*

		KR1_T612_2	OL-PVA3	Initial Average	Final
TDS	(g/L)	23.8	4.8	9.0	9.0
pH		8.3	7.8	7.9	6.8
pe		-4.6		-4.6	-3.4
HCO_3^-	(mg/L)	20.1	189	152	145
CH_4	(mg/L)	**229**		**50.8**	**0.02**
SO_4^{2-}	(mg/L)	0.84	**370**	**288**	**220**
HS^-	(mg/L)	0.03	0.03	0.03	24.2
Fe^{2+}	(mg/L)	0.77	0.03	0.19	0.00
Fe^{3+}	(mg/L)	0.22	0.03	0.02	0.00
Cl^-	(mg/L)	14800	2570	5276	5324
SiO_2	(mg/L)	3.3	11	9.3	9.4
Al^{3+}	(mg/L)	0.06	0.005	0.02	0.02
Na^+	(mg/L)	4800	1290	2067	2086
K^+	(mg/L)	21.0	13.0	14.8	14.9
Ca^{2+}	(mg/L)	4000	390	1189	1166
Mg^{2+}	(mg/L)	56.0	108	96.4	97.4

Table 4-4. *From start of operation to 100 years. Constant input TDS 9 g/L. Constant temperature 45°C in the tunnel unit. Groundwater flow rate 1,500 l/yr.*

	Constant Input	**Final Output**	**Total Mass Transfer in Unit Volume for 150,000 Litres H_2O**		
Years	**0**	**100**			
pH	6.8	7.5			
pe	-3.4	-3.9			
	mg/L	**mg/L**		**mol**	**kg**
HCO_3^-	145	68	ΔHCO_3^-	529	32.3
SO_4^{2-}	220	215	ΔSO_4^{2-}	2088	200.6
HS^-	24.2	0.0	ΔHS^-	-110	-3.6
Fe(tot)	0.0	0.0	ΔFe(tot)	0.3	0.02
Cl^-	5327	5326	ΔCl^-	-1583	-56.1
SiO_2	9.4	12.4	ΔSiO_2	7.3	0.4
Na^+	2085	3217	ΔNa^+	9751	224
K^+	14.9	62.9	ΔK^+	212	8.3
Ca^{2+}	1166	219	ΔCa^{2+}	-3398	-136
Mg^{2+}	97.5	40	ΔMg^{2+}	-143	-3.5

4.1.3 From closure until the next glaciation

This phase has been divided into four time steps due to the different conditions (salinity levels and temperatures) as shown in Table 4-2. Mass-balance results during these time steps are discussed below.

From 100 to 200 years after the beginning of repository operations

After 100 years of activities the repository is closed and the flow rates through the tunnel unit slow down significantly. Otherwise the conditions in the first deposition tunnel are assumed to stay similar to the operational stage. The salinity of infiltrating groundwater is assumed to stay at level of 9 g/L and the temperature in the middle of the first deposition tunnel is estimated to stay at 45°C. It is assumed the post-closure transient conditions will take 100 years from the repository closure.

During the post-closure transient conditions the water inflow from the reserves of sea-water related meteoric water and up-coned saline water continues. The water salinity is at same level as in the operational stage. The water composition flowing into the tunnel unit is presented in Table 4-3. Otherwise, the amounts of reactive solids taken into account in the calculations are inherited from the final calculation output of the operational stage.

During the 100-years of transient conditions little happens in the tunnel unit. Because hydraulic flow slows down to 10 L/year, only 1,000 litres (1 m^3) of water flow through the tunnel unit. This small amount compared to the tunnel unit size.

The results of mass-transfer calculations are presented in Table 4-5. The active solids and processes are similar as in the previous stage with the exception of gypsum that was dissolved completely from the tunnel unit during the operational stage. Since the diffuse layers upon clay surfaces were equilibrated to the 9 g/L of water salinity during the previous stage, no mass-transfer actions in the diffuse layer is expected to occur. This condition can be verified from the no-mass transfer result of Cl^- (Table 4-5). Na-montmorillonite continues to release Na^+ and entrap Ca^{2+}.

During the simulated 100-year time-span the tunnel unit looses a little its Na-montmorillonite character. However, these changes occur before the last calculation cell (cell #29, cf. Fig. 3-1). By the end of simulation calculations, Na-montmorillonite composition is still untouched in the last calculation cell.

According to Table 4-5, some microbially mediated sulphate reduction occurs within the tunnel unit (0.04 mol precipitated) this reaction contributes 0.08 mol of HCO_3^- to bicarbonate net-mass balance (cf. Eq. 3-2). The 0.7 mol precipitation of HS^- indicates that 1.4 mol of goethite has dissolved from the tunnel unit reserves.

Table 4-5. *From 100 years to 200 years. Constant input TDS 9 g/L. Constant temperature 45°C in the tunnel unit. Groundwater flow rate 10 l/yr.*

	Constant Input	Final Output	Total Mass Transfer in Unit Volume for 1,000 Litres H_2O		
Years	**100**	**200**			
pH	6.8	7.5			
pe	-3.4	-3.9			
	mg/L	**mg/L**		**mol**	**kg**
HCO_3^-	145	68	ΔHCO_3^-	1.8	0.11
SO_4^{2-}	220	215	ΔSO_4^{2-}	-0.04	-0.004
HS^-	24.2	0.0	ΔHS^-	-0.7	-0.02
Fe(tot)	0.0	0.0	ΔFe(tot)	0.0	0.0
Cl^-	5327	5326	ΔCl^-	-0.4	-0.02
SiO_2	9.4	12.4	ΔSiO_2	0.05	0.0
Na^+	2085	3217	ΔNa^+	23.6	0.54
K^+	14.9	63	ΔK^+	0.8	0.03
Ca^{2+}	1166	219	ΔCa^{2+}	-11.6	-0.46
Mg^{2+}	97.5	40	ΔMg^{2+}	-0.6	-0.01

From 200 to 5,000 years after the beginning of repository operations

During 200–5,000 years, after the beginning of repository operations, the average salinity and temperature within the first deposition tunnel are set to 8 g/L and 35°C, respectively (Table 4-2). The site-scale hydrological simulations indicate that both salinity and temperature are constantly and slowly decreasing with time (Table 4-1). In the mass-transfer calculations it is assumed that the 8 g/L salinity is a result of mixing of two water types. The brackish water component is taken from the final output of the previous simulation stage (Table 4-5). In the course of time this 9 g/L water is diluted with meteoric water. Meteoric water composition used for dilution was taken from the database of actual samplings of Olkiluoto site (Table 4-6). Furthermore, it is assumed that a constant flux of methane from deeper layers of the bedrock continues to replenish the brackish sulphate containing water at the repository depth. In Table 4-6, this metastable condition is presented with significant concentrations of both sulphate and methane in the same brackish sample. The conservative initial mixing result of the two reference waters are presented in the column “Initial Average”. This water experiences the microbially mediated methane oxidation and results the “Final” input water for the simulation. Due to methane manipulation method, the total HS^- concentration is at a high level in the “Final” input water. The “Initial Average” input water contains already 21 mg/L HS^- before methane oxidation. Methane oxidation almost doubles the HS^- concentration (42 mg/L) in the “Final” input water. The HS^- concentration at this level is a conservative maximum estimate of potential hydrogen sulphide concentrations after repository closure.

The total mass-transfers between 200 and 5,000 years from the beginning of repository operations are presented in Table 4-7. Due to slow flow rate (10L/year) through the tunnel unit, only 48,000 litres (48 m^3) of water comes out from the 5.5-metre section of tunnel backfill in the studied time-span.

Table 4-6. *Compilation of model input water with salinity of 8 g/L (see Table 4-2). The initial waters have been chosen from the constant input water of the previous simulation stage (9 g/L) and from Posiva's OIVA (OL-PVP5A/1) database. It is assumed that more saline component receives a constant gas flux of methane from depth (approx. 78 ml/L(H_2O) at NTP). The initial average water is a weighted sum. The final average input water has been modified from the initial average with methane oxidation reaction coupled with calcite and pyrite equilibria.*

		Water 9 g/L	OL-PVP5A/1	Initial Average	Final
TDS	(g/L)	9.0	0.51	8.0	8.0
pH		7.9	7.6	7.9	6.8
pe		-4.6		-4.6	-3.5
HCO_3^-	(mg/L)	145	329	166	143
CH_4	(mg/L)	**50.8**		**44.8**	**0.04**
SO_4^{2-}	(mg/L)	**220**	**31.0**	**198**	**138**
HS^-	(mg/L)	24.2	0.00	21.3	42.3
Fe^{2+}	(mg/L)	0.000	0.00	0.00	0.00
Fe^{3+}	(mg/L)	0.000	0.00	0.00	0.00
Cl^-	(mg/L)	5324	4.3	4697	4736
SiO_2	(mg/L)	9.4	24.0	11.1	10.9
Al^{3+}	(mg/L)	0.02	0.01	0.02	0.02
Na^+	(mg/L)	2086	19.0	1842	1856
K^+	(mg/L)	14.9	8.3	14.1	14.3
Ca^{2+}	(mg/L)	1166	76.0	1038	1005
Mg^{2+}	(mg/L)	97.4	19.0	88.1	88.9

Table 4-7. *From 200 years to 5,000 years. Constant input TDS 8 g/L. Constant temperature 35°C. Groundwater flow rate 10 L/yr.*

	Constant Input	**Final Output**	**Total Mass Transfer in Unit Volume for 48,000 Litres H_2O**		
Years	**200**	**5,000**			
pH	6.8	6.6			
pe	-3.5	-2.6			
	mg/L	**mg/L**		**mol**	**kg**
HCO_3^-	143	223	ΔHCO_3^-	115.9	7.1
SO_4^{2-}	138.1	65.6	ΔSO_4^{2-}	-21.7	-2.1
HS^-	42.3	0.0	ΔHS^-	-61.4	-2.0
Fe(tot)	0.0	0.19	ΔFe(tot)	0.2	0.0
Cl^-	4718	4713	ΔCl^-	198	7.0
SiO_2	10.9	9.0	ΔSiO_2	-1.5	-0.1
Na^+	1856	2375	ΔNa^+	1231	28.3
K^+	14.1	41	ΔK^+	34.5	1.3
Ca^{2+}	1005	552	ΔCa^{2+}	-496	-19.9
Mg^{2+}	89.0	65	ΔMg^{2+}	-37.7	-0.9

When the simulation starts, the pores of the tunnel volume are filled with final water of the previous simulation (see Table 4-5), and cation occupation in the exchange sites are as equilibrated within the previous simulation. Similarly, all solid phase amounts available for equilibrium and kinetic reactions are inherited from the previous simulation.

During the simulation, small amounts of several species are flushed out from the unit volume. Initially (at year 200), the system is filled with the clearly brackish (9 g/L, cf. Table 4-3) water and all solid phases within the unit volume are essentially equilibrated with this water. This means that about 11,600 L (11.6 m^3) of highly brackish water is flushed out from the system almost without any mass transfer during the simulation of first 1,200 years, the time it takes for a water parcel to flow through the unit cell (5.5 metres long). However, the difference between the 9 g/L and 8 g/L waters is relatively small.

According to Table 4-7, a portion of Na^+ extracted from the unit volume comes conservatively out with the initial 9 g/L brackish water. The tunnel unit clay is still mostly Na-montmorillonite, and consequently cation exchange towards mixed (Na,Ca)-montmorillonite is still active process. Additionally, the higher charged cations (i.e. Ca^{2+}, Mg^{2+}) prefer exchange sites more because of solute dilution (Appelo & Postma 1996). This phenomenon promotes Na^+ (and K^+) flush out from the system. At later stages the situation becomes balanced. More Na^+ is taken into exchange sites and some calcite dissolves. At the end of simulation, the molar ratios of cations within the last calculation cell (cell #29) are slightly changed from the final stage of the earlier simulation: NaX = 0.76, CaX_2 = 0.17, MgX_2 = 0.05, and KX = 0.02.

As the more saline brackish water is flushed out from the tunnel backfill, a part of Cl^- comes out from the system. As it was pointed out earlier, the diffuse layers upon the clay surfaces are active in the calculations as well. As the input water becomes more dilute, the diffuse layers become gradually more dilute as well.

Input water carries high concentrations of hydrogen sulphide. All HS^- is precipitated as pyrite within the tunnel backfill as a result of simultaneous goethite dissolution. Moreover, sulphate reduction occurs within the system as a result of organic activity. The sulphate level of the input water drops to about half during the infiltration through the tunnel unit. The resulting dissolved hydrogen sulphide precipitates as pyrite. The sulphate concentration never reaches thermodynamic equilibrium as long as there is sulphate within the input water, and goethite and organic matter are available within the solid phases. Pyrite production into backfill in this way is rate limited by organic activity. It is worth noting that according to Equation (3-2) every reduced mole of sulphate produces two moles of bicarbonate. This means that about 43 moles from the total positive flux of bicarbonate (116 moles) can be attributed to organic activity (Table 4-7).

From 5,000 to 10,000 years after the beginning of operations

During 5,000–10,000 years after the beginning of repository operations, the average salinity and temperature within the mid-part of the first deposition tunnel are set to 5

g/L and 28°C, respectively. Both values are still slowly dropping as a function of time but the gradients are already quite gentle.

The 5 g/L brackish water located at the repository depth is generated from the previous stage brackish 8 g/L water by diluting it with the meteoric water used already in the previous simulation stage (Table 4-8). It is assumed that the brackish sulphate-containing water is constantly contaminated with a methane gas flux from deeper depths. Since the water contains hydrogen sulphide already, the additional contribution as a result of methane oxidation leads to a quite high hydrogen sulphide concentration (37 mg/L) in the "Final" input water. Once again this concentration must be considered as a quite conservative maximum estimate of potential hydrogen sulphide concentrations.

The net-mass-transfers for the time span 5,000–10,000 years after the beginning of repository operations are presented in Table 4-9. During 5,000 years 50,000 litres (50 m^3) of water infiltrates through the tunnel unit.

Similarly to the previous stage calculations, the simulation starts with the slow flush-out of higher saline 8 g/L water out from the tunnel unit. After 11,600 litres of water have run through the tunnel unit, water has changed within the tunnel unit to the lower salinity 5 g/L brackish water.

The summary (Table 4-9) indicates that among major cations changes in mass-balances do occur. A large fraction of Na^+ is flushed out from the system at an early stage of simulation. The diffuse double layers begin to dilute as a response of more dilute input water. At the beginning of the simulations the montmorillonite composition within backfill is still far away from the mixed (Na,Ca)-montmorillonite composition. Exchange between Na^+ and Ca^{2+} continues during the simulation, and the process releases Na^+ in the solution.

As in the stage before, at early stages of simulation divalent cations tend to prefer exchange sites as solute concentration decreases. The net-effect is that Ca^{2+} is retarded at a small extent in the tunnel backfill, while the other major cations are released. At the end of simulation the exchanger site occupations, in the last calculation cell (cell #29), are approaching the mixed (Na,Ca)-montmorillonite equilibrium, i.e. NaX = 0.59, CaX_2 = 0.30, MgX_2 = 0.09, and KX = 0.02. It is worth noting that compared to previous stages, the cation ratios in the input water are not markedly changed because the brackish water is repeatedly diluted with low-ionic-strength meteoric water.

As in the simulation step above, the more saline brackish water (8 g/L) is flushed out from the tunnel unit and replaced with lower saline brackish water (5 g/L). Mostly due to this process a moderate amount of Cl^- is flushed out from the system. As indicated at earlier stages, the goethite in the tunnel unit is capable to precipitate all hydrogen sulphide as pyrite from the input water. Likewise, as in the earlier simulation step, microbially mediated sulphate reduction produces roughly same amount of hydrogen sulphide in the porewater that is in turn precipitated as pyrite, as well. Microbially mediated sulphate reduction produces also bicarbonate (42 moles) into the porewater, and it is carried mostly out from the tunnel unit within outflow water.

Table 4-8. *Compilation of model input water with salinity of 5 g/L (see Table 4-2). The initial waters have been chosen from the constant input water of the previous simulation stage (8 g/L) and from Posiva's OIVA (OL-PVP5A/1) database. It is assumed that more saline component receives a constant gas flux of methane from depth (approx. 69 ml/L(H_2O) at NTP). The initial average water is a weighted sum. The final average input water has been modified from the initial average with methane oxidation reaction coupled with calcite and pyrite equilibria.*

		Water 8 g/L	OL-PVP5A/1	Initial Average	Final
TDS	(g/L)	8.0	0.51	5.0	5.0
pH		7.9	7.6	7.8	6.9
pe		-4.6		-4.6	-3.6
HCO_3^-	(mg/L)	143	329	218	181
CH_4	(mg/L)	**44.8**		**26.9**	**0.10**
SO_4^{2-}	(mg/L)	**138**	**31.0**	**95**	**61.2**
HS^-	(mg/L)	42.3	0.00	25.4	37.3
Fe^{2+}	(mg/L)	0.00	0.00	0.00	0.00
Fe^{3+}	(mg/L)	0.00	0.00	0.00	0.00
Cl^-	(mg/L)	4736	4.3	2839	2854
SiO_2	(mg/L)	10.9	24.0	16.2	16.2
Al^{3+}	(mg/L)	0.02	0.01	0.01	0.01
Na^+	(mg/L)	1856	19.0	1120	1126
K^+	(mg/L)	14.3	8.3	11.9	11.9
Ca^{2+}	(mg/L)	1005	76.0	633	596
Mg^{2+}	(mg/L)	88.9	19.0	60.9	61.2

Table 4-9. *From 5,000 years to 10,000 years. Constant input TDS 5 g/L. Constant temperature 28°C. Groundwater flow rate 10 L/yr.*

	Constant Input	**Final Output**	**Total Mass Transfer in Unit Volume for 50,000 Litres H_2O**		
Years	**5,000**	**10,000**			
pH	6.9	7.0			
pe	-3.6	-3.0			
	mg/L	**mg/L**		**mol**	**kg**
HCO_3^-	181	237	ΔHCO_3^-	131	8.0
SO_4^{2-}	61.2	11.0	ΔSO_4^{2-}	-18.2	-1.7
HS^-	37.3	0.0	ΔHS^-	-56.5	-1.9
Fe(tot)	0.0	0.12	ΔFe(tot)	0.26	0.01
Cl^-	2826	2826	ΔCl^-	624	22.1
SiO_2	16.2	7.2	ΔSiO_2	-7.5	-0.5
Na^+	1126	1532	ΔNa^+	1304	30.0
K^+	11.9	24.8	ΔK^+	20.6	0.8
Ca^{2+}	596	271	ΔCa^{2+}	-292	-11.7
Mg^{2+}	61.2	30.4	ΔMg^{2+}	-41.9	-1.0

From 10,000 to 13,000 years after the beginning of operations

The simulation is continued seamlessly from the previous stage except for a change in temperature (see Table 4-2). The input water composition remains similar as tabulated in Table 4-8 but the temperature is different. The previous stage simulated 5,000 years while at this stage mass-transfers occurring during 3,000 years are predicted.

Because the input water composition is the same as the output water from the previous stage there is practically no mass-transfer related to chloride, and no adjustments in the diffuse double layer composition. As in the previous simulation, the constant input water contains a high concentration of hydrogen sulphide (Tables 4-8 and 4-10). However, all dissolved sulphide is precipitated as pyrite within the tunnel backfill unit as a result of iron oxyhydroxide dissolution. The microbially mediated sulphate reduction contributes also a solid amount of hydrogen sulphide for iron coprecipitation as pyrite.

Table 4-10 indicates that, in addition to organic carbon dissolution, calcite dissolution occurs in the tunnel unit and HCO_3^- is being constantly contributed into output water. The balances among the major cations indicate that Ca^{2+} is retarded into cation exchange. Because the constant input water composition, the mass-balance among the major cations is almost stoichiometric. Na^+ and K^+ are released (497 mols total), and Ca^{2+} and Mg^{2+} are retarded (243 mols total). The slight imbalance should be attributed to calcite equilibrium. Cation exchange is still ongoing within the tunnel unit. However, within the last calculation cell (cell #29) the changes are small and the exchanger site occupations there are almost the same as at end of the previous stage ($NaX = 0.40$, $CaX_2 = 0.53$, $MgX_2 = 0.06$, and $KX = 0.02$).

During the modelled 3,000 years of infiltration, 30,000 litres (30 m^3) of water runs through the studied tunnel unit. The complete pore volume in the tunnel unit is 11,600 litres (11.6 m^3). During the modelled time-span water is changed within the tunnel unit approximately 2.5 times.

Table 4-10. *From 10,000 years to 13,000 years. Constant input TDS 5 g/L. Constant temperature 23°C. Groundwater flow rate 10 L/yr.*

	Constant Input	**Final Output**	**Total Mass Transfer in Unit Volume for 30,000 Litres H_2O**		
Years	**10,000**	**13,000**			
pH	6.9	6.8			
pe	-3.6	-2.8			
	mg/L	**mg/L**		**mol**	**kg**
HCO_3^-	181	324	ΔHCO_3^-	76	4.6
SO_4^{2-}	61.2	9.7	ΔSO_4^{2-}	-14.3	-1.4
HS^-	37.3	0.0	ΔHS^-	-33.9	-1.1
Fe(tot)	0.0	0.25	ΔFe(tot)	0.15	0.01
Cl^-	2826	2826	ΔCl^-	-2.3	-0.1
SiO_2	16.2	7.2	ΔSiO_2	-4.7	-0.3
Na^+	1126	1497	ΔNa^+	488	11.2
K^+	11.9	24.1	ΔK^+	9.4	0.4
Ca^{2+}	596	313	ΔCa^{2+}	-211	-8.5
Mg^{2+}	61.2	34.9	ΔMg^{2+}	-32.3	-0.8

4.1.4 From the onset of the next glaciation until the far future

From 13,000 to 35,000 years, permafrost period

According to the Weichselian-R scenario, the next ice age will begin with permafrost and will continue with a succession of glacial and melting periods. Because of almost no-flow condition from the ground level, the groundwater flow is assumed to slow down at repository depth. This is implemented in the mass-transfer simulation with an almost stagnant condition where the groundwater flow through the tunnel unit is only 1 L/year. At the same time, the groundwater salinity level is three-fold larger than in the previous calculation stage (10,000–13,000 years), as shown in Table 4-2.

It is estimated that a groundwater salinity of 15 g/L would be feasible. More saline water rises gradually upwards from the depth. Therefore, the constant input water was generated from the previous stage constant input (5 g/L) and from a saline sample (25.7 g/L) taken from the database of actual samplings of Olkiluoto site (Table 4-11). The actual sample OL-KR2_596_1 contains only a trace of sulphate but abundant methane. As before, the final constant input water was generated by assuming that bacteria oxidate methane, and reduces sulphate. This lowers the concentrations levels of methane and sulphate, but raises the dissolved sulphide concentrations. The resulting water composition after equilibration with calcite and pyrite is presented in Table 4-11.

The final water composition coming out from the tunnel unit after a 22,000-year-simulation is presented in Table 4-12. The final output resembles, with few exceptions, closely the input water composition. The main differences are distinctly grown Fe^{2+} and Mg^{2+} concentrations, and around three times higher bicarbonate and K^{+} concentrations in the final output water. The final water coming out from the tunnel is essentially free of dissolved sulphide and sulphate.

The mass-transfers predicted to occur in the backfill unit volume are presented in Table 4-12. During 22,000 years of infiltration total 22,000 litres (22 m^3) of water comes out from the other end of the tunnel unit. This means that water is changed almost twice in the tunnel backfill unit during the modelled time-span corresponding to a very slow flow rate.

Major compositional changes occur within the backfill. Compared to the previous stage, the three times higher salinity causes entrapment of major cations and anions within the backfill. This means salinity rise within the diffuse double layers (DDL) of the clay surfaces. The clay surfaces are expected to be negatively charged. In the calculated conditions, the clay surfaces attract primarily cations. However, major cations participate also to cation exchange. Therefore, compositional change within the DDL is primarily manifested with the entrapment of chlorine.

Because input water salinity rises significantly, it can be expected that in the cation exchange the selectivity between cation charges is lost (e.g. Appelo & Postma 1996, Stumm 1992). This lost of selectivity is not, however, directly observable because at the same time significant amount of cations are retarded within DDL. Anyway, calculations indicate that the both major cations (Na^{+} and Ca^{2+}) are entrapped within the backfill, while the less dominant cations (K^{+} and Mg^{2+}) are flushed out, at some extent, from the backfill unit.

Table 4-11. *Compilation of model input water with salinity of 15 g/L (Table 4-2). The initial waters have been chosen from the constant input water of the previous simulation stage (5 g/L) and from Posiva's OIVA (OL-KR2_596_1) database. According to measurements, the more saline component is in equilibrium with a gas phase containing methane approx. 386 ml/L(H_2O) at NTP. The initial average water is a weighted sum. The final average input water has been modified from the initial average with methane oxidation reaction coupled with calcite and pyrite equilibria.*

		Water 5 g/L	KR2_596_1	Initial Average	Final
TDS	(g/L)	5.0	25.7	15.0	15.0
pH		7.9	9.1	8.5	6.9
pe		-4.6	-5.5	-5.0	-3.7
HCO_3^-	(mg/L)	181	7.0	96.8	61.1
CH_4	(mg/L)	**26.9**	**252**	**136**	**0.13**
SO_4^{2-}	(mg/L)	**61.2**	**1.3**	**32.3**	**16.1**
HS^-	(mg/L)	37.3	0.1	19.4	25.4
Fe^{2+}	(mg/L)	0.00	0.01	0.00	0.00
Fe^{3+}	(mg/L)	0.00	0.00	0.00	0.00
Cl^-	(mg/L)	2854	16000	9197	9336
SiO_2	(mg/L)	16.2	0.7	8.7	8.9
Al^{3+}	(mg/L)	0.01	0.01	0.01	0.01
Na^+	(mg/L)	1126	4750	2874	2918
K^+	(mg/L)	11.9	18.0	14.9	15.1
Ca^{2+}	(mg/L)	596	4800	2625	2633
Mg^{2+}	(mg/L)	61.2	38.0	50.0	50.8

Table 4-12. *From 13,000 years to 35,000 years. Constant input TDS 15 g/L. Constant temperature 23°C. Groundwater flow rate 1 L/yr.*

	Constant Input	**Final Output**	**Total Mass Transfer in Unit Volume for 22,000 Litres H_2O**		
Years	**13,000**	**35,000**			
pH	6.9	6.6			
pe	-3.7	-2.7			
	mg/L	**mg/L**		**mol**	**kg**
HCO_3^-	61.1	182	ΔHCO_3^-	77.6	4.7
SO_4^{2-}	16.1	0.04	ΔSO_4^{2-}	-3.4	-0.3
HS^-	25.4	0.0	ΔHS^-	-16.9	-0.6
Fe(tot)	0.0	3.1	ΔFe(tot)	0.7	0.04
Cl^-	9261	9261	ΔCl^-	-2143	-76.0
SiO_2	8.9	5.6	ΔSiO_2	-1.1	-0.1
Na^+	2918	2978	ΔNa^+	-766	-17.6
K^+	15.1	51.6	ΔK^+	11.8	0.5
Ca^{2+}	2633	2222	ΔCa^{2+}	-763	-30.6
Mg^{2+}	50.8	263	ΔMg^{2+}	88.5	2.2

The positive bicarbonate net mass-transfer indicates that a certain amount of calcite is dissolved in the simulation. The dissolved bicarbonate is flushed out from the tunnel unit, while part of the dissolved Ca^{2+} is taken into cation exchange and within the DDL's.

Negative mass-transfers related to sulphate and sulphide indicates that the small concentrations coming in with the input water are reacted and precipitated as pyrite within the tunnel backfill.

From 35,000 to 125,000 years, ice sheet and submerged periods

After the formation of permafrost, Olkiluoto will be either under a continental ice sheet or below interglacial sea levels until the climate becomes temperate again and the site emerges from the sea by land uplift. For both the continental ice sheet state and the submerged state, no-flow conditions are assumed to exist from ground level to the repository level because overlying extensive ice sheet or sea do not generate any effective hydraulic gradients. Because of continental ice sheet melting, high hydraulic gradient conditions are predicted at the ice margin. According to simulations, however, the ice margin withdraws relatively fast if long-lived cold weather periods do not stop the withdrawal. It is predicted that, without these additional delays, the withdrawing ice margin will pass Olkiluoto within less than 100 years. This time is so short that significant melt water intrusion does not take place at repository depth.

In the mass-transfer simulations, flow conditions are practically stagnant and the groundwater flow through the tunnel unit is 0.5 L/year. This extremely low flow condition at repository depth is prolonged and, based on hydrological modelling results, it is assumed that the groundwater salinity rises to a level of 25 g/L. This water is made up by mixing the previous stage 15 g/L water and the actual Olkiluoto sample OL-KR2_596_1 that has salinity 25.7 g/L. The actual sample defines the 25 g/L water composition almost completely. The final input water is presented in Table 4-13 and it contains practically no methane and very little dissolved sulphate and sulphide.

The final output water simulated to emerge from the other end of the tunnel unit is presented in Table 4-14. The final output water results after 90,000 years of simulation and after 45 m^3 of water has run through the tunnel unit. During the simulation time, water has changed almost four times within the tunnel unit (the complete pore volume is 11.6 m^3). The composition of the final output water resembles in places the constant input water. However, bicarbonate concentration has grown to a high level while compared to the input. The Fe^{2+} and Mg^{2+} concentrations have grown around ten fold levels in the output. Similarly, the K^+ level is around four times higher. There is no dissolved sulphur in the output.

As in the previous stage (13,000–35,000 years) significant changes occur within the solid phases of the backfill. The salinity of input water is almost doubled and this causes a salinity rise within the DDL's of the backfill material. As in the previous case, the salinity increase within the DDL is shown with otherwise conservative entrapment of Cl^-.

The input water is strongly saline. The molar Na/Ca ratio within the constant input water is 1.7, while in the final output the ratio is 1.6. These numbers indicate that the selectivity between cation charges is minimal in the cation exchange. As in the previous case, calculations show that both major cations (Na^+ and Ca^{2+}) are entrapped within the backfill, but the flush-out of less dominant cations (K^+ and Mg^{2+}) continues.

Table 4-13. *Compilation of model input water with salinity of 25 g/L (Table 4-2). The initial waters have been chosen from the constant input water of the previous simulation stage (15 g/L) and from Posiva's OIVA (OL-KR2_596_1) database. According to measurements, the more saline component is in equilibrium with a gas phase containing methane approx. 386 ml/L(H_2O) at 20°C and 1 atm. The initial average water is a weighted sum. The final average input water has been modified from the initial average with methane oxidation reaction coupled with calcite and pyrite equilibria.*

		Water 15 g/L	KR2_596_1	Initial Average	Final
TDS	(g/L)	15.0	25.7	25.0	25.0
pH		8.5	9.1	9.1	7.8
pe		-5.0	-5.5	-5.5	-4.8
HCO_3^-	(mg/L)	96.8	7.0	13.1	5.5
CH_4	(mg/L)	**136**	**252**	**245**	**0.08**
SO_4^{2-}	(mg/L)	**32.3**	**1.3**	**3.3**	**0.43**
HS^-	(mg/L)	19.4	0.12	1.4	2.5
Fe^{2+}	(mg/L)	0.00	0.01	0.00	0.00
Fe^{3+}	(mg/L)	0.00	0.00	0.00	0.00
Cl^-	(mg/L)	9197	16000	15541	15936
SiO_2	(mg/L)	8.7	0.7	1.2	1.2
Al^{3+}	(mg/L)	0.01	0.01	0.01	0.01
Na^+	(mg/L)	2874	4750	4623	4741
K^+	(mg/L)	14.9	18.0	17.8	18.2
Ca^{2+}	(mg/L)	2625	4800	4653	4766
Mg^{2+}	(mg/L)	50.0	38.0	38.8	39.8

Table 4-14. *From 35,000 years to 125,000 years. Constant input TDS 25 g/L. Constant temperature 20°C. Groundwater flow rate 0.5 L/yr.*

	Constant Input	**Final Output**	**Total Mass Transfer in Unit Volume for 45,000 Litres H_2O**		
Years	**35,000**	**125,000**			
pH	7.8	6.5			
pe	-4.8	-2.7			
	mg/L	**mg/L**		**mol**	**kg**
HCO_3^-	5.5	146	ΔHCO_3^-	119	7.2
SO_4^{2-}	0.4	0.01	ΔSO_4^{2-}	-0.1	-0.01
HS^-	2.5	0.0	ΔHS^-	-3.4	-0.1
Fe(tot)	0.0	7.3	ΔFe(tot)	5.0	0.3
Cl^-	15869	15869	ΔCl^-	-2182	-77.3
SiO_2	1.2	4.7	ΔSiO_2	2.7	0.2
Na^+	4741	4126	ΔNa^+	-1789	-41.1
K^+	18.2	74.6	ΔK^+	58.3	2.3
Ca^{2+}	4766	4521	ΔCa^{2+}	-950	-38.1
Mg^{2+}	39.8	512	ΔMg^{2+}	762	18.5

According to calculations slight calcite dissolution occurs during the simulated time-span as it has continued through the simulated future scenario. However, there is still abundant calcite within the backfill. Similarly, sulphate reduction, and consequently the sulphide precipitation consume constantly iron oxyhydroxide reserves within the backfill. It seems however, that reserves are large enough to handle the mass-transfers considered.

During the glacial melting period(s), the repository may experience high flow rates. Oxidizing conditions are possible if extensive melt water intrusion occurs and flushes out of higher salinity water with more dilute water. However, based on the hydrological simulation results, the assumption is that these glacial melting periods are too short to affect the geochemistry at the repository depth. Moreover, the available groundwater geochemical data indicate that only around 10% mixing of glacial melt water has occurred at the repository depth in the more or less known history of Olkiluoto. This melt water contribution is possibly only partially from the latest Weichselian deglaciation (cf. Pitkänen et al. 2004, p. 118, and Luukkonen et al. 2005, p. 28).

4.2 Emissions-M scenario

4.2.1 Input data from site-scale groundwater flow modelling

This scenario is similar to the Weichselian-R scenario for the first 10,000 years. Afterwards, this climate scenario is characterized by a continuous land uplift and dilution of groundwater salinities as a function of time. Input data from 0 to 10,000 years from the beginning of repository operations is the same as for the Weichselian-R scenario (Table 4-1) and therefore they are not repeated here. The essential results for the unit cell extracted from the site-scale groundwater flow calculations are presented in Table 4-15.

Table 4-15. *Data imported from site-scale groundwater flow calculations (Posiva 2007). Time from the beginning of depositions, Darcy velocities, TDS concentrations, and temperature. Results refer to the Emissions-M scenario.*

Time (yr)	Calculated Darcy velocity (m/yr)	Flow through an tunnel area of 14 m^2 (l/yr)	TDS (g/l)	Temperature (°C)
0-10,000	As in the Weichselian-R scenario (Table 4-1)			
10,000	$1.1 \cdot 10^{-6}$	0.015	4.1	25.8
20,000	$7.6 \cdot 10^{-7}$	0.011	1.4	20.0
30,000	$8.5 \cdot 10^{-7}$	0.012	0.7	20.0
40,000	$8.2 \cdot 10^{-7}$	0.011	0.4	20.0
50,000	$7.8 \cdot 10^{-7}$	0.011	0.2	20.0

For the modelling of the geochemical mass-balances, the chosen flow rates in the tunnel and the chosen TDS concentrations at different time periods for the Emissions-M scenario are presented in Table 4-16. The same reasoning has been used to adjust the flow rates from the site-scale groundwater flow calculations (multiplied by 1,000) are applied here as in the Weichselian-R scenario.

Table 4-16. *Time periods from start of operation, the chosen flow rates in the tunnel and TDS concentrations for the Emissions-M scenario. Until 10,000 years the input data are the same as in the Weichselian-R scenario (Table 4-2).*

Time frame	Time (years after beginning of depositions)	Groundwater flow rate for the tunnel (l/yr)	TDS concentration (g/L)	Temperature in the backfill (°C)
Operational phase	0-100	As in the Weichselian-R scenario		
From closure until the next glaciation	100-5,000	As in the Weichselian-R scenario		
	5,000-10,000	As in the Weichselian-R scenario		
	10,000-20,000	10	3	23
	20,000-100,000	10	0.51	20

4.2.2 From closure until the next glaciation

According to "greenhouse" climate predictions (Posiva 2007) it will take at least 100,000 years until the next glaciation will occur. Therefore, the Emissions-M scenario continues after 10,000 years with uplift and groundwater dilution. The time steps considered are 10,000-20,000 years and 20,000-100,000 years.

From 10,000 to 20,000 years after the beginning of operations

According to hydrological simulations deep groundwater at the repository depth are already dilute brackish in composition (Table 4-15). In the mass-transfer calculations it is estimated that the average TDS concentration and temperature in deep groundwater are 3 g/L and 23°C, respectively (see Table 4-16).

The predicted 3 g/L groundwater is generated by diluting the previous stage 5 g/L input water (Table 4-8) with the meteoric 0.51 g/L meteoric water (Table 4-17). In addition to dissolved sulphate and constant methane flux from depth, the initial 5 g/L water contains remarkable amount of dissolved hydrogen sulphide. As a result of mixing dilution with meteoric water and simultaneous methane oxidation reaction the final input water contains relatively small amount of sulphate and still quite high amount of dissolved hydrogen sulphide (24 mg/L). This is considered as a maximum estimate of hydrogen sulphide concentration potentially infiltrating into the tunnel backfill.

The total mass-transfers assumed to occur during years 10,000–20,000 years after the beginning of repository operations are presented in Table 4-18. During these 10,000 years, 100,000 litres (100 m^3) of water infiltrates through the tunnel backfill unit.

Table 4-17. *Compilation of model input water with salinity of 3 g/L (see Table 4-16). The initial waters have been chosen from the constant input water of the previous simulation stage (5 g/L) and from Posiva's OIVA (OL-PVP5A/1) database. It is assumed that more saline component receives a constant gas flux of methane from depth (approx. 25 ml/L(H_2O) at NTP). The initial average water is a weighted sum. The final average input water has been modified from the initial average with methane oxidation reaction coupled with calcite and pyrite equilibria.*

		Water 5 g/L	OL-PVP5A/1	Initial Average	Final
TDS	(g/L)	5.0	0.51	3.0	3.0
pH		7.9	7.6	7.8	6.9
pe		-4.6		-4.6	-3.7
HCO_3^-	(mg/L)	181	329	240	202
CH_4	(mg/L)	**26.9**		**16.1**	**0.17**
SO_4^{2-}	(mg/L)	**61.2**	**31.0**	**49.1**	**30.9**
HS^-	(mg/L)	37.3	0.00	22.4	28.8
Fe^{2+}	(mg/L)	0.00	0.00	0.00	0.00
Fe^{3+}	(mg/L)	0.00	0.00	0.00	0.00
Cl^-	(mg/L)	2854	4.3	1712	1717
SiO_2	(mg/L)	16.2	24.0	19.3	16.2
Al^{3+}	(mg/L)	0.01	0.01	0.01	0.01
Na^+	(mg/L)	1126	19.0	682	684
K^+	(mg/L)	11.9	8.3	10.5	10.5
Ca^{2+}	(mg/L)	596	76.0	388	356
Mg^{2+}	(mg/L)	61.2	19.0	44.3	44.4

Table 4-18. *From 10,000 years to 20,000 years. Constant input TDS 3 g/L. Constant temperature 23°C. Groundwater flow rate 10 L/yr.*

	Constant Input	**Final Output**	**Total Mass Transfer in Unit Volume for 100,000 Litres H_2O**		
Years	**10,000**	**20,000**			
pH	6.9	7.3			
pe	-3.7	-3.4			
	mg/L	**mg/L**		**mol**	**kg**
HCO_3^-	202	206	ΔHCO_3^-	156	9.5
SO_4^{2-}	30.9	2.5	ΔSO_4^{2-}	-27.3	-2.6
HS^-	28.8	0.0	ΔHS^-	-87.0	-2.9
Fe(tot)	0.0	0.05	ΔFe(tot)	0.25	0.01
Cl^-	1691	1691	ΔCl^-	375	13.3
SiO_2	16.2	6.1	ΔSiO_2	-16.9	-1.0
Na^+	684	984	ΔNa^+	1643	37.8
K^+	10.5	15.8	ΔK^+	16.7	0.7
Ca^{2+}	356	130	ΔCa^{2+}	-500	-20.1
Mg^{2+}	44.4	14.4	ΔMg^{2+}	-111.4	-2.7

Table 4-18 indicates that lower charged cations are flushed out form the system, while higher charged cations are retarded in the tunnel backfill. Like in the earlier stage (from 5,000 to 10,000 years), during the first 1,200 years there occurs significant flushing of more saline brackish water out of the tunnel unit. At the end of this time-span, the porewater salinity has dropped from 5 g/L to 3 g/L. As before, the higher charged cations prefer exchange sites, due to dilution, at the beginning of simulation. However, also the molecular rates within the input water are changed slightly as well. By the end of simulation, the cationic ratios within the exchanger of the last calculation cell (cell # 29) are: NaX = 0.40, CaX_2 = 0.50, MgX_2 = 0.09, and KX = 0.01.

Water dilution at the beginning of the simulation is indicated with the flushing out of Cl^- from the unit cell with no change in final input and output concentrations.

Similarly to the previous stages, significant HS^- concentration within the input water are all precipitated as pyrite with the aid of goethite dissolution. After 20,000 years abundant reserves of goethite are still available within the tunnel unit to cause precipitation. Similarly to previous stages as well, significant amount of the SO_4^{2-} content from the input water is reduced to HS^- with the aid of microbial activity. The precipitated amount of SO_4^{2-} indicates that the related microbial activity has produced about 55 moles HCO_3^- to the positive bicarbonate mass-balance. All HS^- produced in the sulphate reduction is also precipitated as pyrite within the tunnel unit, like in the earlier stages.

From 20,000 to 100,000 years after the beginning of operations

It is predicted that after 20,000 years the groundwater TDS at the repository depth will correspond fresh water composition (Table 4-15). In the current calculations it is assumed that the fresh water composition in the far future is similar to the fresh water sample (OL-PVP5A/1) utilised in the earlier calculations (cf. Tables 4-6, 4-8, and 4-17). The estimated TDS concentration and temperature at repository depth are 0.51 g/L and 20°C, respectively.

The fresh water sample (OL-PVP5A/1) shown in Tables 4-6, 4-8, and 4-17 contains small amounts of dissolved sulphate. Although, it can be assumed that this water will be contaminated with methane gas flux from deeper depths, this option was not used in the calculations. As earlier calculations indicate, sulphate levels are relatively effectively lowered by organic activity within the tunnel backfill. After the microbially mediated sulphate reduction, the pyrite precipitation is similar process compared to methane oxidation (that is microbially mediated as well).

The constant fresh water composition infiltrates into the tunnel backfill unit for 80,000 years. During this time-span, 800,000 litres (800 m^3) of fresh water flows through the unit. Considering the time, it can be concluded that the amount of water interacting with the backfill is still relatively low in terms of litres per year (10 L/year).

According to Table 4-19, the similar trend with the major cations continues as in the earlier simulation stages (Tables 4-7, 4-9, and 4-18). The montmorillonite yields slightly more Na^+ into porewater and binds little more Ca^{2+} from porewater than in the earlier stages. The cationic ratio within the input water is different as compared to input waters

of earlier stages. In the 10,000–20,000-year simulation (cf. Table 4-18) the molar Na/Ca input ratio was 3.3, but in the current simulation this ratio is 0.43 in the input water. Moreover, the general dilution of water is expected to retard higher charged ions within the montmorillonite. By the end of simulation, the cationic ratios within the exchanger of the last calculation cell (cell #29) have altered slightly and are: NaX = 0.39, CaX_2 = 0.51, MgX_2 = 0.09, and KX = 0.01.

As it can be expected the dilution of input water TDS results the flush out porewater with higher TDS. This process is shown with Cl^- flush out from the tunnel unit.

During 80,000 years of simulation, 223 mol of sulphate precipitate within the tunnel unit. According to Equation (3-2), this means that 446 mol of bicarbonate is released into porewater and is flushed out from the tunnel unit. As indicated in Table 4-19, a majority of bicarbonate increase within the output water results from this organic activity. Again like in the earlier simulations, sulphate reduction produces hydrogen sulphide that is precipitated as pyrite while the necessary iron is taken from goethite dissolution.

Table 4-19. *From 20,000 years to 100,000 years. Constant input TDS 0.51 g/L. Constant temperature 20°C.*

	Constant Input	**Final Output**	**Total Mass Transfer in Unit Volume for 800,000 Litres H_2O**		
Years	**20,000**	**100,000**			
pH	7.6	8.4			
pe	-2.8	-4.5			
	mg/L	**mg/L**		**mol**	**kg**
HCO_3^-	329	366	ΔHCO_3^-	552	33.7
SO_4^{2-}	31.0	5.5	ΔSO_4^{2-}	-223	-21.4
HS^-	0.0	0.0	ΔHS^-	0.0	0.0
Fe(tot)	0.0	0.0	ΔFe(tot)	0.0	0.0
Cl^-	21.2	21.2	ΔCl^-	955	33.9
SiO_2	24.0	5.7	ΔSiO_2	-244	-14.7
Na^+	19.0	148	ΔNa^+	5340	123
K^+	8.3	2.4	ΔK^+	-112	-4.4
Ca^{2+}	76.0	4.2	ΔCa^{2+}	-1386	-55.6
Mg^{2+}	19.0	0.5	ΔMg^{2+}	-599	-14.5

4.3 Main uncertainties in mass balance calculations

The presented calculations are first attempt to calculate geochemically coupled cumulative mass balances in a tunnel unit. The first results therefore are fraught with uncertainties and cannot yet be used to draw meaningful conclusions on the processes taking place at the repository macro-scale or at the unit cell scale.

One of the main uncertainties of these calculations is the actual groundwater flow rate in the repository tunnel. According to safety regulations there should not be advective flow within the backfill. However, to study the geochemical equilibria in the backfill the

groundwater flow rate from the site-scale groundwater flow modelling calculations has been multiplied by 1000.

Additional uncertainties are carried over from the site-scale groundwater flow model results on salinity levels and temperatures in the backfill. The overall uncertainty around the development of the swelling pressure in the buffer and backfill also affects the calculations. If cracks or flow pathways are formed in the backfill, minerals could precipitate in these cracks soon after the beginning of repository operation. From the modelling point of view, the material homogeneity is lost both if cracks are formed and if such cracks are partially or completely filled by precipitated minerals. In such cases, lumped parameters for heterogeneous materials should be used. Also, if groundwater pathways are formed in the backfill, transport occurs via advection and no longer via diffusion. Also, short-term tests (Karnland et al. 2000) indicate that the heat-induced cracking within the deposition hole is a real process, but no data is available on the long-term behaviour of such cracks, although the expectation is that such cracks would close upon saturation of the buffer.

There may be further uncertainties linked to the reaction mechanisms, rate constants, and equilibrium constants used in the calculation of porewater chemistry both in the buffer and in the backfill.

Current calculations indicate that there is a pronounced tendency for dissolved sulphide precipitation within the tunnel backfill because of bentonite mineralogy. This feature should be confirmed experimentally, and if needed, the future modelling attempts should take more thoroughly into account the reaction rate factors related to this process. Furthermore, the microbial-mediated sulphate reduction rate utilised in the calculations is an estimate and is based on only the few values available from literature.

It is crucial for canister-scale modelling that macro-scale predictions on future repository evolution are credible. As an example, in the current Weichselian-R scenario, glacial stages in the far future contain glacial melting stages. In the calculations these stages were assumed to be short lived and it was further postulated that melting stages do not affect at the repository depth. However, this is not exactly what seem have happened in history during the Weichselian deglaciation. According to observations (Pitkänen et al. 2004, Luukkonen et al. 2005) glacial melt waters have penetrated to the repository depth.

The geochemical modelling of the tunnel unit is affected by several issues pending resolution or further experimental and/or modelling data. Examples of such issues are the following:

- impact of structural changes in the backfill (e.g. precipitated minerals within cracks) on the hydraulic conductivity and swelling pressure;
- reversibility of e.g. salinity changes to the backfill and to swelling pressures;
- impact of cementitious materials on geochemical mass balances within the unit cell;
- impact of diluted water intrusion on bentonite during the glacial melting period.

5 CONCLUSIONS

These preliminary results reveal qualitative trends for mass balances in a final repository tunnel unit. Already during the operational period (when parts of the repository are open) the exchange sites of montmorillonite alter in composition significantly. However, in the whole tunnel unit montmorillonite in the bentonite backfill changes completely from sodium-bentonite to mixed sodium-calcium-bentonite only after about 10,000 years. After this conversion (NaX/CaX_2) the composition of the mixed montmorillonite seems to change only within narrow limits.

Saline waters affect the swelling pressure of the tunnel backfill in two ways. Firstly, the conversion from Na-montmorillonite to (Ca,Na)-montmorillonite lowers the swelling pressure of the bentonite. Secondly, saline waters affect the diffuse double layer (DDL) thickness within the bentonite. The more saline the porewater the narrower are the DDL's. The narrower DDL's result in a lower swelling pressure. The Weichselian-R scenario results after 10,000 years show that the backfill gradually become a larger sink for Cl^- as the porewater becomes more saline. In the Emissions-M scenario the opposite may be predicted. Porewater becomes more and more dilute with time, and it can be assumed that the swelling pressures due to the dilution of the diffuse layer in montmorillonite, increases as the salinity decreases (see Fig. 3-2).

With regard to SO_4^{2-} and HS^-, the preliminary results show that all HS^- produced within or coming into contact with the bentonite of the deposition tunnel backfill is readily precipitated as pyrite within the backfill. Considering specifically the simulated tunnel unit, the simulation calculations indicate that there are enough reserves of ferro-oxyhydroxides to dissolve and precipitate all available HS^- species as pyrite within the tunnel backfill during the first 100,000 years. All iron-oxyhydroxide required for this reaction is contributed by the 30% bentonite part of the backfill. The iron-oxyhydroxide content within the 70% crushed rock is conservatively assumed to be zero. The ferro-oxyhydroxide reserves of bentonite are important issue considering the sulphur cycle. The issue should be confirmed experimentally.

Within the tunnel unit, bicarbonate is produced from organic matter oxidation coupled with sulphate reduction. Every mole of sulphate produces two moles of bicarbonate. Calculation results (especially in the Emissions-M scenario) show that organic matter oxidation contributes significantly to the dissolved bicarbonate in the final output water. The total inventory of organic matter in the tunnel backfill unit is large (Luukkonen & Nordman 2006) Even assuming that microbes are able to metabolise all types of organic matter the total inventory of organic matter will not be consumed in the considered time-spans.

The mineral buffering capacity of the bentonite in the backfill is long-lived within the unit cell because of the low groundwater flow rate. The water flow through the deposition tunnel has been set to approximately 1,000 times higher than given by the site-scale hydrological simulation results. Despite this exaggeration, the water flow through the tunnel backfill part of the unit cell is very low. Table 5-1 summarises the total volume of water exchanged in the unit cell for each time frame, the total sulphide precipitated and the total bicarbonate contribution from organic matter oxidation. High bicarbonate (HCO_3^-) content in near-neutral pH (6.3–10.3) groundwater is able to buffer

the groundwater against low and high pH attacks as long as a sufficient amount is dissolved in water. The total volume of water infiltrated through the backfill tunnel unit is about 346 m^3 for the Weichselian-R scenario and 1149 m^3 for the Emissions-M scenario. As a comparison, the complete volume of the studied tunnel unit is approximately 77 m^3 (14 m^2 × 5.5 m length). Solid materials in this volume represent approximately 65.4 m^3. In the Weichselian-R scenario the pore volume (i.e. 11.6 m^3) of the tunnel unit is refilled about 30 times during the complete simulation. In the Emissions-M scenario, the tunnel unit is refilled approximately 99 times. These amounts of water are moderate considering the time-spans simulated.

The current study did not consider at all geochemical processes within the canister buffer of the unit cell (se Fig. 2-1). The problems related to the fully-swelled saturated bentonite were introduced shortly in Chapter 2 (e.g. lack of free porewater, and eradication of life). Furthermore, during the thermal pulse bentonite buffer contains water-unsaturated gradients. This is an additional feature that possibly affects if mineral redistribution within the buffer occurs. It can be imagined that an unsaturated cracked in the bentonite allows a vaporisation–condensation cycle to occur. Evidently, knowledge of the life-cycle of buffer bentonite could be improved.

Table 5-1. *Total inventories of selected mass-transfers considered in the simulations.*

Time	Weichselian-R				Emissions-M			
	Total water volume infiltrated	Times tunnel unit refilled	Total sulphide precipitated	Total HCO_3^- contribution from CH_2O	Total water volume infiltrated	Times tunnel unit refilled	Total sulphide precipitated	Total HCO_3^- contribution from CH_2O
(yr)	m^3	#	mol	mol	m^3	#	mol	mol
0-100	150	12.9	110	n.d.	150	12.9	110	n.d.
100-200	1	0.09	1	0.08	1	0.09	1	0.08
200-5,000	48	4.1	83	43	48	4.1	83	43
5,000-10,000	50	4.3	75	36	50	4.3	75	36
10,000-13,000	30	2.6	48	29	100	8.6	114	55
13,000-20,000	22	1.9	20	7				
20,000-35,000					800	69.0	223	446
35,000-100,000	45	3.9	4	0				
100,000-125,000								
Total inventory	**346**	**29.9**	**340**	**116**	**1149**	**99.1**	**605**	**580**
n.d. = not determined								

6 ACKNOWLEDGEMENTS

The drafts of this report were prepared side by side with the manuscript of Posiva Oy's Olkiluoto future evolution report (Posiva 2007). Consequently, several persons have reviewed this working report draft or parts of it during the reparation of the evolution report. We wish to thank especially the evolution report editor Barbara Pastina (SROY) for her work and proposals. Furthermore, Frank Garisto (Ontario Power Generation Inc.), Jari Löfman (VTT), Margit Snellman (SROY), and Nuria Marcos (SROY) have given valuable help and comments to improve the manuscript.

REFERENCES

Appelo, C.A.J. & Postma, D. (1996) Geochemistry, groundwater and pollution. A.A. Balkema, Rotterdam, Netherlands. 536 p.

Börgesson, L & Hernelind, J (1999) Äspö Hard Rock Laboratory. Prototype Repository. Preliminary modelling of the water-saturation phase of the buffer and backfill materials. Swedish Nuclear Fuel and Waste Management Co (SKB), Stockholm, Sweden. International Progress Report 00-11: 99p.

Boudreau, B.P. & Westrich, J.T. (1984) The dependence of bacterial sulfate reduction on sulfate concentration in marine sediments. Geochimica et Cosmochimica Acta 48, 2503–2516.

Bradbury, MH & Baeyens, B (2003) Porewater chemistry in compacted re-saturated MX-80 bentonite. Journal of Contaminant Hydrology 61: 329–338.

Bradbury, MH & Baeyens, B (2002) Porewater chemistry in compacted re-saturated MX-80 bentonite: Physico-chemical characterisation and geochemical modelling. Paul Scherrer Institute, Villingen, Swizerland, PSI Bericht 02-10: 41 p.

Bruno, J, Arcos, D & Duro, L (1999) Processes and features affecting the near field hydrochemistry. Groundwater-bentonite interaction. Swedish Nuclear Fuel and Waste Management Co (SKB), Stockholm, Sweden. Technical Report 99-29: 56 p.

Carslaw, H. S. & Jaeger, J. C. (1959) Conduction of heat in solids. 2nd edition. Clarendon Press, Oxford, U.K.

Cedercreutz, J. (2004) Future climate scenarios for Olkiluoto with emphasis on permafrost. Posiva Oy, Eurajoki, Finland. Report POSIVA 2004-06. 72 p.

Davis, JA & Kent, DB (1990) Surface complexation modeling in aqueous geochemistry. In: (ed. Ribbe, P.H.) Mineral-water interface geochemistry. Mineralogical Society of America, Washington D.C., U.S.A. Reviews in Mineralogy 23: 177–260.

Girguis,P.R. Orphan, V.J., Hallam, S.J. & DeLong, E.F. (2003) Growth and methane oxidation rates of anaerobic methanotropic Archaea in a continuous-flow reactor. Applied and Environmental Microbiology 69(9), 5472–5482.

Koretsky, C.M., Moore, C.M., Lowe, K.L., Meile, C., Dichristina, T.J. & Van Cappellen, P. (2003) Seasonal oscillation of microbial iron and sulfate reduction in saltmarsh sediments (Sapelo Island, GA, USA). Biogeochemistry 64, 179–203.

Luukkonen, A. (2006) Estimations of durability of fracture mineral buffers in the Olkiluoto bedrock. Posiva Oy, Olkiluoto, Finland. Working Report 2006-107. 32 p.

Luukkonen, A. (2004) Modelling approach for geochemical changes in the Prototype repository engineered barrier system. Posiva Oy, Eurajoki, Finland. Working Report 2004-31. 36 p.

Luukkonen, A., Pitkänen, P. & Partamies, S. (2005) Evaluation of Olkiluoto hydrogeochemical data in 3-D – Extended with recent geochemical interpretation results. Posiva Oy, Olkiluoto, Finland. Working Report 2005-72. 71 p.

Luukkonen, A., Pitkänen, P. & Partamies, S. (2004) Significance and estimations of lifetime of natural fracture mineral buffers in the Olkiluoto bedrock. Posiva Oy, Olkiluoto, Finland. Working Report 2004-08. 38 p.

Malmlund, H., Äikäs, K. & Hagros, A. 2004. Layout adaptation examples for a KBS-3V repository at Olkiluoto. Posiva Oy, Olkiluoto, Finland. Posiva Working Report 2003-68.

Nordman, H. & Vieno, T. 2003. Modelling of near-field transport in KBS-3V/H type of repositories with PORFLOW and REPCOM codes. Posiva Oy, Olkiluoto, Finland. Posiva Working Report 2003-07. 66 p.

Parkhurst, D.L. & Appelo, C.A.J. (1999) User's guide to PHREEQC (Version 2) – A computer program for speciation, batch-reaction, one-dimensional transport, and inverse geochemical calculations. U.S. Geological Survey, Denver, Colorado. Water-Resources Investigations Report 99-4259: 312 p.

Pirhonen, V (1986) Bentoniittitäyteaineen ominaisuudet. Puristetun bentoniitin koostumus ja fysikaaliset ominaisuudet – koe-erä R11-85 (unpubl. report in Finnish). Teollisuuden Voima Oy, Eurajoki, Finland. TVO/KPA – Turvallisuus ja tekniikka, Work Report 86-03: 6 p.

Pitkänen, P., Partamies, S. & Luukkonen, A. (2004) Hydrogeochemical interpretation of baseline groundwater conditions at the Olkiluoto site. Posiva Oy, Olkiluoto, Finland. Report POSIVA 2003-07. 160 p.

Posiva (2007) Expected evolution of a spent fuel repository at Olkiluoto. Posiva Oy, Helsinki, Finland. Report POSIVA 2006-05. 412 p.

Posiva (1999) The final disposal facility for spent nuclear fuel – Environmental Impact Assessment report. Posiva Oy, Helsinki, Finland.

Poteri, A. & Laitinen, M. (1999) Site-to-canister scale flow and transport at the Hästholmen, Kivetty, Olkiluoto and Romuvaara sites. Posiva Oy, Helsinki, Finland. Report POSIVA 99-15. 156 p.

Roychoundhury, A.N., Van Cappellen, P., Kostka, J.E. & Viollier, E. (2003) Kinetics of microbially mediated reactions: Dissimilatory sulfate reduction in saltmarsh sediments (Sapelo Island, Georgia, USA). Estuarine, Coastal and Shelf Science 56, 1001–1010.

Roychoundhury, A.N., Viollier, E. & Van Cappellen, P. (1998) A plug flow-through reactor for studying biogeochemical reactions in undisturbed aquatic sediments. Applied Geochemistry 13, 269–280.

SKB (2005) Äspö Hard Rock Laboratory. Annual Report 2004. Swedish Nuclear Fuel and Waste Management Co (SKB), Stockholm, Sweden. Technical Report TR-05-10. 211 p.

Stumm, W. (1992) Chemistry of the solid-water interface. John Wiley & Sons, Inc., New York, U.S.A. 428 p.

Valentine, D.L. & Reeburgh, W.S. (2000) New perspectives on anaerobic methane oxidation. Environmental Microbiology 2(5), 477–484.

Van Cappellen, P. & Wang, Y. (1996) Cycling of iron and manganese in surface sediments: A general theory for the coupled transport and reaction of carbon, oxygen, nitrogen, sulfur, iron, and manganese. American Journal of Science 296(3), 197–243.

Viollier, E.S., Jézéquel, D. & Sarazin, G. (2000) Determination of sulfate reduction kinetics in Aydat lake sediments. American Society for Limnology and Oceanography. Summer Meeting, June 5-9, Copenhagen, Denmark.

Vuorinen, U., Lehikoinen, J., Luukkonen, A. & Ervanne, H. (2003) Effects of salinity and high pH in crushed rock and bentonite - experimental work and modelling in 2001 and 2002. Posiva Oy, Eurajoki, Finland. Working Report 2003-22, 33 p.

Wieland, E, Wanner, H, Albinsson, Y, Wersin, P & Karnland, O (1994) A surface chemical model of the bentonite-water interface and its implications for modelling the near field chemistry in repository for spent fuel. Swedish Nuclear Fuel and Waste Management Co (SKB), Stockholm, Sweden. Technical Report 94-26: 64 p.